Food and Chemical Toxicology 132 (2019) 110672

Contents lists available at ScienceDirect

Food and Chemical Toxicology

journal homepage: www.elsevier.com/locate/foodchemtox

Phenolic compounds from coffee by-products modulate adipogenesis-related inflammation, mitochondrial dysfunction, and insulin resistance in adipocytes, via insulin/PI3K/AKT signaling pathways

Miguel Rebollo-Hernanz[a,b,c], Qiaozhi Zhang[c,d], Yolanda Aguilera[a,b], Maria A. Martín-Cabrejas[a,b,**], Elvira Gonzalez de Mejia[c,*]

[a] Institute of Food Science Research, CIAL (UAM-CSIC), 28049, Madrid, Spain
[b] Department of Agricultural Chemistry and Food Science, Universidad Autónoma de Madrid, 28049, Madrid, Spain
[c] Department of Food Science and Human Nutrition, University of Illinois at Urbana-Champaign, IL, 61801, United States
[d] College of Food Science, Northeast Agricultural University, Harbin, 150030, China

ARTICLE INFO

Keywords:
Coffee by-products
Inflammation
Insulin resistance
Mitochondrial dysfunction
Phenolic compounds

ABSTRACT

The aim of this study was to evaluate the inhibitory potential of aqueous extracts from coffee silverskin (CSE) and husk (CHE) and their main phenolics on adipogenesis, obesity-related inflammation, mitochondrial dysfunction, and insulin resistance, *in vitro*. Coffee by-products extracts (31–500 μg mL^{-1}) and pure phenolics (100 μmol L^{-1}) reduced lipid accumulation and increased mitochondrial activity in 3T3-L1 adipocytes. Also reduced the expression of inducible nitric oxide synthase and cyclooxygenase-2 and diminished secretion of pro-inflammatory factors in LPS-stimulated RAW2643.7 macrophages. Cytokine release diminished (tumor necrosis factor α: 23–57%; monocyte chemoattractant protein 1: 42–60%; interleukin-6: 30–39%) and adiponectin increased (7–13- fold) in adipocytes treated with macrophage-conditioned media. ROS scavenging and activation of peroxisome proliferator-activated receptor γ coactivator 1-α pathway counteracted mitochondrial dysfunction. Increases in insulin receptor (1.4 to 4-fold), phosphoinositide 3-kinase (2 to 3-fold) and protein kinase B (1.3 to 3-fold) phosphorylation, in conjunction with a decrease in serine phosphorylation of insulin receptor substrate 1, evoked glucose transporter 4 translocation (8–15-fold) and glucose uptake (44–85%). CSE and CHE phenolics inhibited adipogenesis and elicited adipocytes browning. Suppressing macrophages-adipocytes interaction alleviated inflammation-triggered mitochondrial dysfunction and insulin resistance. CSE and CHE are beneficial in reducing adipogenesis and inflammation-related disorders.

1. Introduction

Overweight and obesity are defined as excessive fat accumulation that may impair health and are triggered by excessive energy storage as triglycerides (TAG) in adipose tissue (AT). About 13% of the adult world population is obese; a major risk factor for chronic diseases including type-2 diabetes (T2D) (Paniagua, 2016). Obesity is associated with a state of low-grade chronic inflammation that leads to impairment of insulin signaling (Monteiro and Azevedo, 2010). Insulin resistance (IR) is associated with an increased number of infiltrated macrophages (Mφ) in the AT, which promotes the secretion of cytokines and other inflammation-related factors (Jung and Choi, 2014). AT, as an endocrine organ, secretes adipocytokines as leptin, adiponectin, tumor necrosis factor α (TNF-α), interleukin 6 (IL-6), and monocyte chemoattractant protein 1 (MCP-1) (Kang et al., 2016). Inflammatory cytokines induce lipolysis in adipocytes, and the release of free fatty acids (FFAs) activates inflammatory signals in both Mφ and adipocytes creating an inflammatory paracrine loop (Suganami et al., 2005).

Mitochondria have a fundamental function in energy metabolism producing energy for the cells in the form of adenosine triphosphate (ATP) from food substrates (Brand et al., 2013). Obesity-related inflammation has been shown to alter the number and function of mitochondria in different tissues, resulting in mitochondrial dysfunction (Patti and Corvera, 2010). Mitochondrial dysfunction in adipocytes induces the loss of insulin sensitivity and hinders insulin response and glucose utilization in other tissues, leading to a decrease in adiponectin secretion (Wang et al., 2013). The perturbation in mitochondrial

* Corresponding author. 228 ERML, 1201 West Gregory Dr. Urbana, IL 61801, United States.
** Corresponding author. Instituto de Investigación en Ciencias de la Alimentación, Calle Nicolás Cabrera, 9, 28049, Madrid, Spain.
E-mail addresses: miguel.rebollo@uam.es (M. Rebollo-Hernanz), maria.martin@uam.es (M.A. Martín-Cabrejas), edemejia@illinois.edu (E. Gonzalez de Mejia).

https://doi.org/10.1016/j.fct.2019.110672
Received 30 March 2019; Received in revised form 24 June 2019; Accepted 10 July 2019
Available online 12 July 2019

oxidative metabolism may affect the electron transport chain, causing an electron flow towards oxygen and production of superoxide and other reactive oxygen species (ROS) (Jastroch et al., 2010). Reduced oxidation of fatty acids, fuels of mitochondria, causes lipid accumulation (Murphy, 2009). Mφ-secreted factors and an increase in intracellular ROS may activate inhibitor of kappa B kinase (IKK)/nuclear factor kappa-light-chain-enhancer of activated B cells (NF-κB). In addition, Jun N-terminal kinase (JNK)/mitogen-activated protein kinase (MAPK) signaling, blocking insulin signaling via serine phosphorylating and inactivation of insulin receptor substrate-1 (IRS-1) (Zhang et al., 2016). As a result, phosphoinositide 3-kinase (PI3K)/protein kinase B (AKT) signaling pathway is arrested, inhibiting insulin-stimulated glucose transporter 4 (GLUT4) translocation to the cell membrane and glucose uptake (Lumeng et al., 2007; McArdle et al., 2013). Hence, the blockade of the interplay Mφ-adipocytes emerges as an appealing target to reduce inflammation-related consequences of obesity, mitochondrial dysfunction, and IR.

In this regard, phenolic compounds, consumed as part of the diet, could be considered as a preventive nutritional strategy for diminishing the prevalence of obesity and related chronic disorders (Aguilera et al., 2016). Coffee by-products, including coffee husk and silverskin, are generated in large amounts during coffee harvesting and processing and are generally settled to the environment causing ecological problems (Janissen and Huynh, 2018). They contain noteworthy amounts of antioxidant compounds, including phenolics, that could be recovered for their use as value-added products (del Castillo et al., 2019; Dorsey and Jones, 2017). In this sense, coffee by-products have been recently verified as safe food ingredients (Iriondo-DeHond et al., 2018). Phenolic compounds from coffee by-products, primarily chlorogenic acid (CGA), have demonstrated *in vitro* and *in vivo* potential to ameliorate the symptoms of T2D by increasing insulin secretion by β-cells and protecting the pancreas from oxidative stress (Fernandez-Gomez et al., 2016a, 2016b).

The anti-inflammatory potential of coffee by-products on AT and the molecular mechanisms of action have not been characterized to date. The present research aimed to evaluate the inhibitory action of aqueous extracts from coffee silverskin and coffee husk, and their pure phenolic compounds, on adipogenesis, obesity-related inflammation, and derived mitochondrial dysfunction and insulin resistance *in vitro*. We hypothesized that phenolic compounds present in these extracts could exert an anti-inflammatory effect in both Mφ, by inhibiting their activation, and on adipocytes, by decreasing adipogenesis, regulating adipokine secretion, ROS production, and modulating insulin resistance through the alleviation of mitochondrial dysfunction.

2. Materials and methods

2.1. Materials

Dulbecco's modified Eagle medium (DMEM) was obtained from Corning Cellgro® (Manassas, VA), fetal bovine serum (FBS), newborn calf serum (NBS), penicillin-streptomycin (100×) and 0.25% trypsin-EDTA were purchased from Gibco Life Technologies (Grand Island, NY). Pure phenolic compounds (purity ≥ 96%) including chlorogenic acid (CGA, 3-caffeoylquinic acid), caffeic acid (CA), protocatechuic acid (PCA), gallic acid (GA), and kaempferol (KMP) were purchased from Sigma-Aldrich (St. Louis, MO). Anti-mouse inducible nitric oxide synthase (iNOS, PA1-036) primary antibody was acquired from Thermo Fisher Scientific (Rockford, IL). Anti-mouse cyclooxygenase-2 (COX-2, sc-19999), glyceraldehyde 3-phosphate dehydrogenase (GAPDH, sc-47724), peroxisome proliferator-activated receptor γ coactivator 1-α (PGC-1α, sc-518025), and uncoupling protein 1 (UCP1, sc-293418) primary antibodies were obtained from Santa Cruz Biotechnology (CA, USA). All other chemicals and reagents were obtained from Sigma-Aldrich (St. Louis, MO) unless otherwise specified.

2.2. Preparation and UPLC-ESI-MS/MS characterization of the aqueous phenolic extracts from coffee by-products

Coffee silverskin from Colombia was provided by Fortaleza S.A. (Spain) and coffee husk by "Las Morenitas" (Nicaragua) both from the Arabica species. Based on preliminary and optimized extraction protocols, phenolic aqueous extracts from coffee by-products were prepared (Aguilera et al., 2019). These methods were statistically optimized using a Box-Behnken response surface experimental design and the optimal conditions (time, temperature, solid-to-solvent ratio) for the extraction of the maximum concentration of phenolic compounds were employed. After milling and sieving, ground coffee silverskin (25 g) was added into 500 mL of boiling water (100 °C) and stirred for 10 min. Coffee husk (10 g) was added into boiling water (500 mL) and stirred for 90 min. Coffee silverskin aqueous extract (CSE) and coffee husk aqueous extract (CHE) were filtered and freeze at −20 °C for 24 h. Extracts were freeze-dried and stored at −20 °C until further use. The analysis of targeted phenolic compounds was carried out by UPLC-ESI–MS/MS following the method described by Sánchez-Patán et al. (2011). Dissolved extracts were filtered (0.22 μm) and internal standard 4-hydroxybenzoic-2,3,5,6-d4 acid solution (Sigma-Aldrich, St. Louis, MO) was added to the samples in a proportion 1:5 (v/v). For the quantification, data were collected under the multiple reaction monitoring mode, tracking the specific transition of parent and product ions for each compound. The ESI was operated in negative ionization mode. All compounds were quantified using the calibration curves of their corresponding standards.

2.3. Cell culture

The mouse 3T3-L1 preadipocytes and RAW264.7 Mφ (ATCC, Rockville, MD, USA) cell lines were cultured in DMEM containing 10% (v/v) NBS/FBS, respectively, and 1% (v/v) antibiotics, and maintained at 37 °C in a humidified atmosphere containing 5% CO_2.

2.3.1. Adipocyte differentiation

3T3-L1 preadipocytes were cultured in DMEM with 1.5 g L^{-1} sodium bicarbonate, supplemented with 10% (v/v) NBS and 1% (v/v) antibiotics. Subcultured cells ($6{\cdot}10^3$ cells cm^{-2}) were differentiated into adipocytes following the protocol outlined by Zebisch et al. (2012). At day 10–12, cells were completely differentiated and used for the experiments.

2.3.2. Experimental design

Experiments were conducted as follows:

2.3.2.1. Determination of the impact on adipogenesis and lipolysis. CSE, CHE (31–500 μg mL^{-1}), and pure compounds (100 μmol L^{-1}) were added at each media refeed during the differentiation process until adipocytes reached 10–12 days of differentiation. Cells and supernatants were collected and stored at −80 °C until further analysis.

2.3.2.2. Evaluation of the inhibition of Mφ. RAW264.7-Mφ were seeded at $7{\cdot}10^4$ cells cm^{-2} density. Cells were treated for 24 h with LPS (1 μg mL^{-1}) in the presence/absence of CSE, CHE (31–500 μg mL^{-1}), and pure compounds (100 μmol L^{-1}). Cells and supernatants were collected and stored at −80 °C until further analysis.

2.3.2.3. Study of the inflammatory loop between Mφ. Fully differentiated adipocytes (in day 10–12 of the differentiation process) were incubated for 24 h in the presence or absence of Mφ-conditioned media (CM) obtained after LPS-stimulation (1 μg mL^{-1}) of Mφ for 24 h, and CSE, CHE (31–500 μg mL^{-1}), or pure compounds (100 μmol L^{-1}). Cells and supernatants were collected and stored at −80 °C until further analysis. Treatment concentrations were selected based on preliminary data and our previous research. Coffee by-products extracts and pure compounds

showed no *in vitro* cyto/genotoxicity nor *in vivo* toxicity in concentrations within the range of this study, displaying positive effects both in cell culture and animals (Fernandez-Gomez et al., 2016a; Iriondo-DeHond et al., 2018, 2017; Rebollo-Hernanz et al., 2019).

2.3.3. Cell viability

Cell viability of cells treated with CSE, CHE (31–500 μg mL^{-1}), and pure compounds (100 μmol L^{-1}) was performed with the CellTiter® 96 Aqueous One Solution Proliferation assay (Promega Corporation, Madison, WI, USA) following manufacturer's instructions.

2.4. Assessment of the effect of coffee by-products aqueous extracts in 3T3-L1 adipocytes on lipid accumulation, lipolysis, and mitochondrial function

2.4.1. Assessment of cellular lipid accumulation

Oil Red O lipid staining was performed as previously described (Luna-Vital et al., 2017). 3T3-L1 cells seeded in 6-well plates and induced to differentiation were treated with CSE, CHE (31–500 μg mL^{-1}), and pure compounds (100 μmol L^{-1}) along the differentiation process. Lipid staining was performed at day 10–12.

2.4.2. Lipolysis evaluation in adipocytes

After a 24 h treatment with CSE, CHE (31–500 μg mL^{-1}), and pure compounds (100 μmol L^{-1}), glycerol was quantified in the culture media using a kit (Cayman Chemical Item No. 10011725). TAG content was determined in cell lysates using a colorimetric assay kit (Cayman Chemical Item No. 10010303). Lipase activity was determined using a lipase activity assay kit (Cayman Chemical Item No. 700640).

2.4.3. Mitochondrial content and activity

Mitochondrial content was determined using Mitotracker Red (Mitotracker Deep Red FM, Invitrogen) measuring fluorescence intensity at excitation and emission wavelengths of 644 nm and 665 nm, respectively. Citrate synthase (CS) activity with a kit (Cayman Chemical Item No. 701040) according to the manufacturer's protocol. The content of the ATP produced was measured in cell lysates using an ATP detection assay kit (Cayman, No. 700410) according to the manufacturer's instructions.

2.5. Evaluation of the effect of coffee by-products aqueous extracts in RAW264.7-Mφ inflammatory activation

2.5.1. iNOS and COX-2 inhibition

Nitric oxide synthase inhibitor screening kit (Fluorometric) (Biovision, Milpitas, CA) was used. Cyclooxygenases-1 and -2 (COX-1 and COX-2) inhibitory activities were measured using a COX inhibitor screening assay following the manufacturer's instructions (Cayman Chemical, Ann Arbor, MI). Diphenyleneiodonium chloride (DDC) was used as a control drug in the inhibition of iNOS.

2.5.2. Determination of inflammatory factors

The amount of nitrite in the supernatant was measured using the Griess reagent following the manufacturer's protocol. Prostaglandin E2 (PGE_2) was measured in the cell culture supernatant using commercially available assays (Life Science Technologies). The procedure was done following the manufacturer's instructions. Cytokines, TNF-α and MCP-1, secretion into the culture media was measured according to the manufacturer's instructions using commercial ELISA kits (R&D systems, Minneapolis, MN, USA).

2.5.3. Detection of intracellular ROS

After treatment with LPS and CSE, CHE (31–500 μg mL^{-1}), or pure compounds (100 μmol L^{-1}) for 24 h, the cells were incubated for 1 h with DMEM and added with DCFDA (25 μmol L^{-1}). RAW264.7 were also stimulated with 100 μM H_2O_2 for 4 h in the presence of CSE, CHE, and pure compounds to test their effects against an oxygen radical, after their incubation with DCFDA (25 μmol L^{-1}) for 1 h. Then, the cells were washed with PBS, and the fluorescence was detected at an excitation/emission wavelength at 485 nm/535 nm, respectively.

2.6. Evaluation of coffee by-products aqueous extracts in the interaction between 3T3-L1 adipocytes and RAW264.7-Mφ

2.6.1. Adipokine and inflammation-induced lipolysis assessment

The amount of adiponectin, MCP-1, IL-6, and TNF-α in the medium was determined using a Milliplex® MAP Mouse Adipocyte Luminex assay by the manufacturer's instructions. The culture media and lysates were tested for glycerol and TAG quantification and lipases activity as described in section *2.4.2*.

2.6.2. Detection of intracellular ROS, mitochondrial superoxide, and mitochondrial membrane potential

ROS production in adipocytes was measured as previously indicated (Section *2.5.4*). Mitochondrial superoxide was detected by incubating treated cells with Mitosox Red (Invitrogen Molecular Probes, Carlsbad, CA, USA) measuring fluorescence at an excitation wavelength of 510 nm and an emission wavelength of 580 nm. Mitochondrial membrane potential (ΔΨm) was determined using the mitochondria-specific fluorescence die, JC-1 (Thermo Fisher, Skokie, IL, USA) following the manufacturer's instruction. JC1 aggregates that were detected at 550/590 nm (excitation/emission), while JC1 monomers were detected at 485/535 nm (excitation/emission). The JC1 ratio aggregates/monomers was calculated for each condition as an indicator of mitochondrial functionality.

2.6.3. Mitochondrial content and activity

The measurement of the mitochondrial content, citrate synthase activity, and ATP content was conducted according to the methods described in section *2.4.3*. Oxygen consumption rate (OCR) is one of the most informative and direct measures of mitochondrial function and was measured using a kit according to the manufacturer's instructions (ab197243; Abcam, Cambridge, UK).

2.6.4. Glucose uptake

The effect of CSE, CHE, and pure compounds in the glucose uptake is measured both through 2-NBDG uptake. 3T3-L1 cells were differentiated in a black 96-well plate with clear bottom and treated with Mφ-CM as previously explained (Section *2.3.3*). Following a 24 h treatment with CSE, CHE, or pure compounds, 100 μmol L^{-1} 2-NBDG was added to cells in glucose-free DMEM and incubated for 1 h. Then the cells were washed with PBS, and the fluorescence was detected at an excitation/emission wavelength of 485/535 nm.

2.6.5. Confocal microscopy of GLUT4 translocation into the membrane

3T3-L1 cells were seeded in an 8-well cultivation chamber for cell culture and immunofluorescence, differentiated, and treated with Mφ-CM as described in Section *2.3.3*. Cells were cultured overnight in low-glucose serum-free DMEM (5.5 mmol L^{-1}) supplemented with 0.25% FBS treated along with CSE, CHE (31–500 μg mL^{-1}), or pure compounds (100 μmol L^{-1}); at the end of the treatment period, cells were starved for 4 h and stimulated with 100 nmol L^{-1} insulin for 30 min. Glucose transporter type 4 (GLUT-4) translocation was determined according to the protocol outlined by Luna-Vital et al. (2017).

2.6.6. Evaluation of the effect of coffee by-products aqueous extracts on the insulin signaling pathway protein phosphorylation

3T3-L1 adipocytes were cultured, differentiated and treated with Mφs-CM in presence/absence of CSE or CHE for 24 h. Then, the cells were serum starved for 30 min followed by insulin-stimulation (1.7 nmol L^{-1} for 10 min). Cell lysates were biotinylated and spread into array slides according to manufacturer's protocol (Insulin Receptor

Phospho Antibody Array, PIG219, Full Moon BioSystems®, Sunnyvale, CA). Results were analyzed as previously described (Luna-Vital et al., 2017).

2.7. Analysis of protein expression by western blot

Cells were washed twice with ice-cold PBS, lysed using the RIPA Lysis Buffer System (Santa Cruz Biotechnology, CA, USA) and centrifuged at 10000 *g*, at 4 °C for 10 min to eliminate cell debris. Protein concentration in the cell lysates was quantified using BSA as a standard by DC protein assay (Bio-Rad, Richmond, CA). Equal quantities of protein samples were separated in 4–20% gradient SDS-polyacrylamide gels (BioRad Laboratories, Inc.) and transferred onto polyvinylidene difluoride membranes. Once blocked with 3% (w/v) nonfat dry milk in 0.1% Tris-buffered saline-Tween 20 (TBST) for 1 h at room temperature, membranes were washed with 0.1% TBST (5 times, 5 min each) and probed with target protein primary antibodies (1:500) overnight at 4 °C. Membranes were rewashed and incubated (2 h, 25 °C) with the anti-IgG horseradish peroxidase-conjugated secondary antibody (1:2500, GE Healthcare, Buckinghamshire, UK). After washing repeated times, bands were detected using the ECL Prime Western Blotting kit (GE Healthcare, Buckinghamshire, UK) and visualized on a GelLogic 4000 Pro Imaging System (Carestream Health, Inc., Rochester, NY, USA). Protein expression was normalized and expressed as relative expression to GAPDH. The ratios of intensities of the particular target protein/GAPDH in each replicated gel were calculated to consider the amount of protein loaded; then, the mean and standard deviation of each of the protein expression ratios was obtained.

2.8. In silico molecular docking

Major phenolic compounds from CSE and CHE were used as potential ligands for enzymes related to adipogenesis, inflammation, mitochondrial function, and IR were evaluated by molecular docking. Crystal structures were obtained from the Protein Data Bank (PDB) (http://www.rcsb.org/pdb/home/home.do). The binding sites of co-crystallized inhibitors or substrates were selected as the center of the docking area. CGA, CA, PCA, GA, and KMP were used as ligands, and their structures were obtained from the PubChem Compound database (https://pubchem.ncbi.nlm.nih.gov/). Ligand gasteiger partial charges were added, and the root of each structure set rotatable bonds detected in AutoDock Tools. Additionally, search space dimensions, center point (Supplementary Table 1), and flexible torsions were also assigned for each protein (Morris et al., 2009). Docking calculations were performed using AutoDock Vina, performing 100 different runs per each ligand. The pose with the highest binding affinity (lowest binding energy) was saved (Trott and Olson, 2010). Protein-ligand interactions and binding modes were visualized in the Discovery Studio 2017 R2 Client (Dassault Systèmes Biovia Corp®). The biological significance of each interaction was obtained from UniProt (https://www.uniprot.org/).

2.9. Bioinformatic analysis

With the resulting differentially expressed proteins, we searched for protein-protein interactions using the STRING database (http://string-db.org) (Szklarczyk et al., 2017). The differentially expressed proteins were categorized based on the biological process and analyzed for Kyoto Encyclopedia of Genes and Genomes (KEGG) pathway enrichment analysis by using the KEGG database (http://www.genome.jp/kegg/kaas/). An interacting network of the studied proteins and their nearest functional and predicted associations was established using STRING.

2.10. Statistical analysis

Samples were prepared and analyzed in triplicate. Results are expressed as the mean ± standard deviation (SD) ($n = 3$) and were assessed statistically by one-way analysis of variance (ANOVA) and *post hoc* Tukey test. Differences were considered significant at $p < 0.05$. The statistical analysis was performed using SPSS 23.0. Non-linear regressions were calculated using GraphPad Prism 7. Multivariate analyses were carried out with XLSTAT 2018 for Microsoft Excel 2016.

3. Results

3.1. Phenolics, mainly protocatechuic acid, from coffee by-products inhibited adipogenesis and elicited adipocyte browning

The UPLC-ESI-MS/MS phenolic profile of CSE and CHE (Supplementary Table 2) showed that chlorogenic acid (CGA, 2.8 mg g^{-1}) and caffeic acid (CA, 0.5 mg g^{-1}) were the main phenolics in CSE, representing 97% of the total phenolic compounds measured. In CHE, the major one was CGA (3.5 mg g^{-1}), but also protocatechuic acid (PCA), kaempferol-3-*O*-galactoside, and gallic acid (GA) were present, accounting 94% of the total amount of studied phenolics, being CA in a less significant concentration. Hence, the main phenolics found among CSE and CHE were selected as pure compounds for subsequent analyses (kaempferol-3-*O*-galactoside was used as aglycone, kaempferol (KMP) since this is the bioavailable form).

None of the treatments, CSE, CHE (31–500 μg mL^{-1}), or pure compounds (100 μmol L^{-1}), exerted cytotoxicity in non-differentiated nor mature 3T3-L1 adipocytes at the concentrations tested ($p > 0.05$) (Supplementary Fig. 1). As shown in Fig. 1, lipid accumulation was decreased by the treatment with the phenolic extracts and their major phenolics significantly ($p < 0.05$), compared with the control. CHE (125 μg mL^{-1}), PCA, and GA (100 μmol L^{-1}) reduced lipid accumulation to a greater extent (37%, 33%, and 28%, respectively) than the other compounds (Fig. 1A). CHE 500 μg mL^{-1} could inhibit more than 50% of lipid accumulation (IC_{50} = 347 μg mL^{-1}) (Fig. 1B). In the same line, aqueous extracts from coffee by-products and pure phenolic compounds increased the release of glycerol in mature adipocytes, thus reducing the content of intracellular TAG (Fig. 1C and D). CSE, CHE, and PCA were the treatments showing the highest potential to increase lipolysis and double glycerol release. This effect was also corroborated by the measurement of total lipase activity, which was significantly increased by PCA treatment (Fig. 1E). Mitochondrial content in 3T3-L1adipocytes was primarily enhanced ($p < 0.05$) by CGA, CA, and PCA (28–33%) ($p < 0.05$; Fig. 1F). A subsequent increase in the activity of the citrate synthase was observed in all the studied treatments (20–43%) (Fig. 1G). Consistently, ATP production increased between 7 and 20% by the treatment of adipocytes with CSE, PCA, and GA (Fig. 1H). Lipid accumulation in adipocytes can also be regulated by modulating fatty acid synthesis. The use of computational chemistry allowed us to observe the interaction of coffee by-products phenolics with enzymes related to these pathways. The strong binding energies (from −5.5 to −8.7 kcal mol^{-1}) suggested a potential implication on the reduction of *de novo* fatty acid synthesis and fat accumulation. (Fig. 1I, Supplementary Table 3). According to results (Fig. 1J), CHE and PCA were the treatments that more noticeably inhibited adipogenesis stimulating adipocyte browning.

3.2. Coffee silverskin and husk phenolics, and kaempferol abrogated LPS-stimulated inflammation in macrophages

Neither CSE and CHE (31–500 μg mL) nor pure compounds (100 μmol L^{-1}) revealed cytotoxic effects in RAW264.7-Mφ at the concentrations tested ($p > 0.05$). CSE, CHE, and pure phenolic compounds significantly inhibited LPS-induced Mφ activation (Fig. 2). LPS-induced expression of both iNOS and COX-2 was reduced by the treatment with CSE and CHE (125 μg mL^{-1}), and their major compounds. The higher ($p < 0.05$) effects were shown for the treatments with KMP, GA, and CGA (Fig. 2A). CSE and CHE compounds interacted

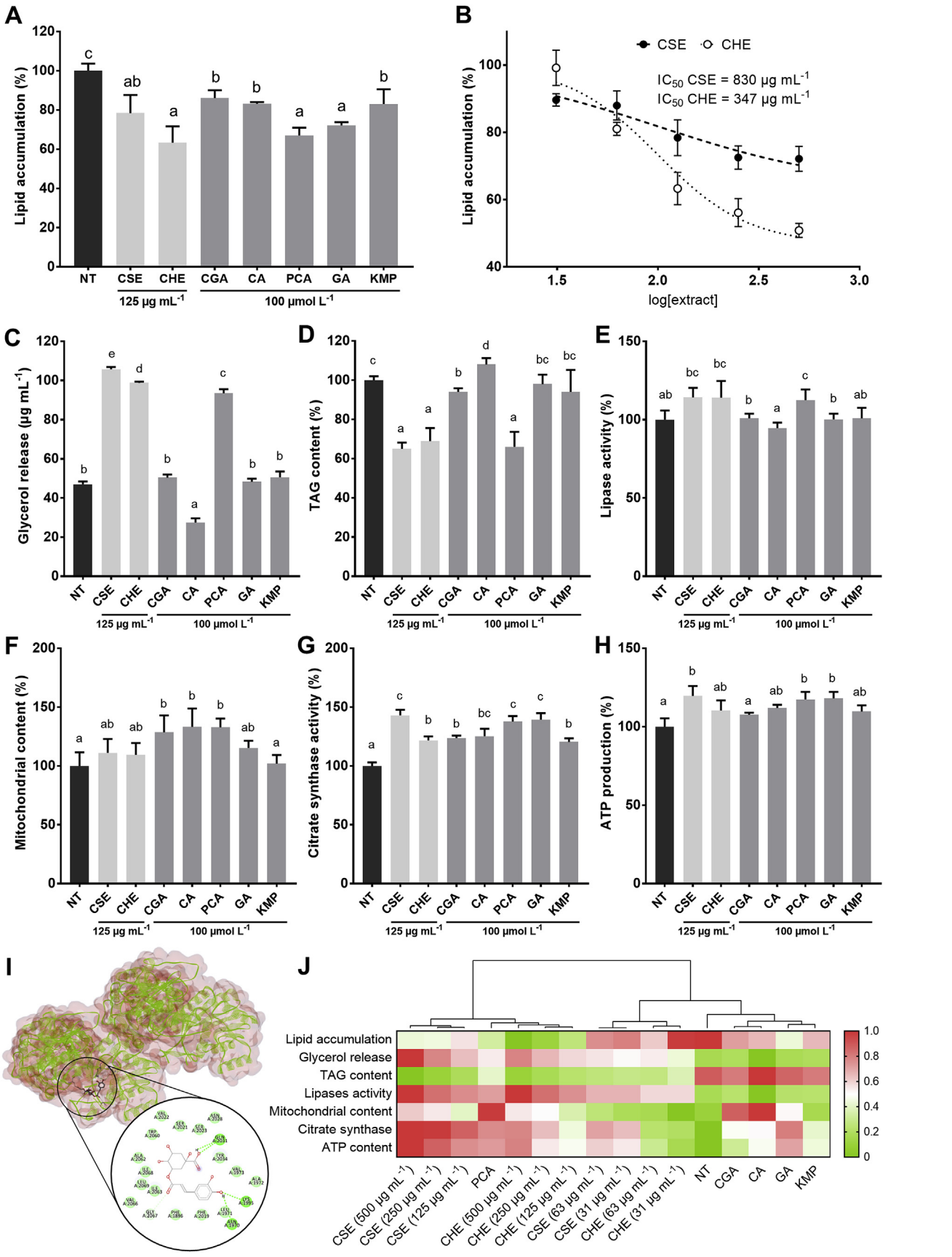

(caption on next page)

Fig. 1. Modulation of lipid accumulation in 3T3-L1 adipocytes determined at the final stage of differentiation (Day 10–12) treated since day 1 with coffee silverskin (CSE) and coffee husk (CHE) aqueous extracts (125 μg mL^{-1}) and pure compounds (100 μmol L^{-1}) (**A**). Dose-dependent inhibition of lipid accumulation (31–500 μg mL^{-1}) (**B**). Effect on lipolysis measured by glycerol release (**C**) intracellular triglycerides content (**D**), and lipase activity (**E**). Impact on mitochondrial content (**F**), citrate synthase activity (**G**), and the production of ATP (**H**). *In silico* interaction of CGA with the reductase domain of the fatty acid synthase protein complex (**I**). Hierarchical cluster analysis and heat map (**J**). The results are expressed as mean ± SD. Bars with different letters significantly ($p < 0.05$) differ according to ANOVA and Tukey's multiple range test. NT: non-treated cells; CGA: chlorogenic acid; CA: caffeic acid: PCA: protocatechuic acid; GA: gallic acid; KMP: kaempferol.

in silico with the catalytic sites of iNOS and COX-2 with binding energies from −6.0 to −9.4 kcal mol^{-1}. These compounds also exhibited high affinity with other pro-inflammatory enzymes (phospholipase A2 and 5-lipooxygenase). These results indicated that besides modulating protein expression, coffee by-products phenolics could also impact enzyme activity (Fig. 2B; Supplementary Table 3). iNOS activity was inhibited at very low concentrations by both CSE and CHE (IC_{50} = 18 and 71 μg mL^{-1}, respectively, versus 1 μg mL^{-1} for the synthetic inhibitor) (Fig. 2C). Similarly, COX-2 was successfully inhibited while the activity of the constitutive COX-1 was inhibited to a lesser extent (IC_{50} COX-2/1 = 8/20 μg mL^{-1} and 35/180 μg mL^{-1}, for CSE and CHE, respectively) (Fig. 2D and E). The levels of the resulting products from the reactions catalyzed by both enzymes (NO and PGE_2) were also modulated (Fig. 2F and G). Both CSE and CHE (31–500 μg mL^{-1}) significant ($p < 0.05$) reduced NO production (13–78%, 42–77%, respectively). GA and KMP reduced NO production dramatically to levels near normal conditions (78 and 99%, respectively). Results demonstrated that CSE was effective in the inhibition of PGE_2 (IC_{50} = 138 μg mL^{-1}). KMP and GA reduced the production of this prostanoid in higher amounts (49 and 84%, respectively) than the other treatments ($p < 0.05$). The release of TNF-α (Fig. 2H) to the cell media was reduced ($p < 0.05$) by all the treatments. Among the pure phenolic compounds, GA and KMP (100 μmol L^{-1}) seemed to be the most potent ones by inhibiting 52 and 100% the secretion of TNF-α. In addition, the levels of MCP-1 in the cell culture media were reduced, following the same trend seen for TNF-α (Fig. 2I). CSE, CHE, and their pure compounds efficiently scavenge ROS indistinctly of the oxidative stress-inductor employed (Fig. 2J and K). CGA and KMP were the most active compounds. Based on the results (Fig. 2L), KMP and CGA seemed to be major contributors to the observed effects of CHE and CSE, respectively, being the effect of KMP to be noteworthy almost completely repressing LPS-inflammatory effects in Mφ.

3.3. Phenolic compounds from coffee by-products modulated the inflammatory paracrine loop macrophages-adipocytes

Fig. 3A shows the reductions of TNF-α release in adipocytes co-treated with Mφ-CM and the extracts and phenolic compounds. The inhibitory effect of CHE on TNF-α production was higher (42%) than that of CSE (31%). Among the phenolic compounds, CGA, PCA, and GA were the most potent ones ($p < 0.05$) (50–57% of TNF-α reduction). Regarding MCP-1 secretion (Fig. 3B), the effects followed similar tendencies; CHE, CGA, and KMP showed a better regulatory effect than the other treatments (57–60% of reduction). Concerning the production of IL-6 (Fig. 3C), all the treatments presented a similar effect. In contrast, CSE, CHE, and their main phenolics avoided the reduction in adiponectin secretion caused by Mφ-CM (Fig. 3D). Treatments promoted its secretion (7–12-fold); the effects of the pure phenolic compounds were higher than those of CSE and CHE (125 μg mL^{-1}) ($p < 0.05$), being CA the most effective one. CM-treated adipocytes exhibited an increased glycerol release (65%) which was partially inhibited by CSE and CHE (31–500 μg mL^{-1}) treatments (7–61% and 19–51%, respectively) (Fig. 3E). The phenolic compounds reduced glycerol release to a lower level than basal conditions. The opposite effects were shown for TAG accumulation (Fig. 3F). Inflammation brought about a decrease in intracellular TAG content whereas the extracts and compounds maintained it. The pure phenolic produced an increase ($p < 0.05$) in TAG content in adipocytes exposed to the Mφ-CM. Fig. 3G shows the reductions in lipase activity in adipocytes treated with CSE, and mainly their composing phenolics. The ability of coffee by-products extracts and their main phenolic compounds to arrest the inflammatory interaction between Mφ and adipocytes seemed to be similar (Fig. 3H).

3.4. Phenolics, mainly chlorogenic acid and kaempferol from coffee by-products, preserved mitochondrial function in adipocytes

Increases in the levels of intracellular ROS resulted from the treatment with Mφ-CM (Fig. 4A). CSE and CHE (31–500 μg mL^{-1}) successfully prevented the inflammation-triggered production of ROS (20–45% and 26–66%, respectively) and mitochondrial superoxide (19–38% and 18–53%, respectively) (Fig. 4B). The treatment with their phenolic compounds (100 μmol L^{-1}) resulted in a higher ($p < 0.05$) scavenging of mitochondrial superoxide. Coffee by-products extracts and pure phenolic compounds partially restored ΔΨm (Fig. 4C), being KMP the most potent compound (91% of the original ΔΨm). Inflammation induced by CM in 3T3-L1 adipocytes reduced PCG-1α and UCP1 protein expression (Fig. 4D). CSE and CHE restored the basal expression of PGC-1α. CGA and KMP elevated PGC-1α protein levels to a higher level in comparison to the non-treated control (20%, 10%, and 39%, respectively). The expression of UCP1 was also enhanced by CSE, CHE, CGA, CA, and KMP. As observed in Fig. 4E, inflammatory factors from Mφ caused a decrease in the total mitochondrial mass, prevented by the treatment of all the extracts and compounds except PCA. Inflammation had a higher impact on mitochondrial function than content (68% CS activity reduction against 26% mitochondrial mass decrease) (Fig. 4F); treatments preserved CS activity, maintaining mitochondrial aerobic capacity in high levels (> 70%). Oxygen consumption rate (OCR) suffered reductions caused by Mφ-CM (Fig. 4G), which were partially inhibited by the treatments with coffee by-products extracts and major phenolic compounds (16–52%). CSE and CHE represed the decrease in ATP synthesis induced by CM (40% and 52%, respectively) and in greater extent phenolic compounds, especially CGA (73%) and KMP (82%) (Fig. 4H). Coffee by-products phenolics demonstrated the ability to interact *in silico* with key enzymes located in mitochondria and expressed in inflammatory conditions. Phenolic compounds interacted with phosphatase-1B (PTP1B), protein-tyrosine phosphatase 1D (SHP-2), and phosphatase and tensin homolog (PTEN). Protein-ligand interaction showed moderate binding energies (−5.5 to −7.9 kcal mol^{-1}) (Fig. 4I; Supplementary Table 3). Hence, adipocytes mitochondrial dysfunction was alleviated by CSE and CHE (Fig. 4J), being CGA and KMP the most active phenolic compounds in both extracts, KMP significantly counteracting CM-triggered mitochondrial dysfunction in adipocytes.

3.5. Coffee by-products aqueous extracts modulated insulin signaling promoting GLUT4 translocation and glucose uptake in adipocytes

Insulin receptor (INSR) signal transduction pathway phosphorylation pattern is summarized in Table 1 and Supplementary Table 4. CSE and CHE significantly ($p < 0.05$) modulated the phosphorylation of a total of 38 and 45 out of 60 proteins, respectively, which were differently phosphorylated in at least one of their phosphorylation sites (accounting a total of 62 and 74 regulated residues, respectively). INSR phosphorylation significantly increased by the treatment with both CSE

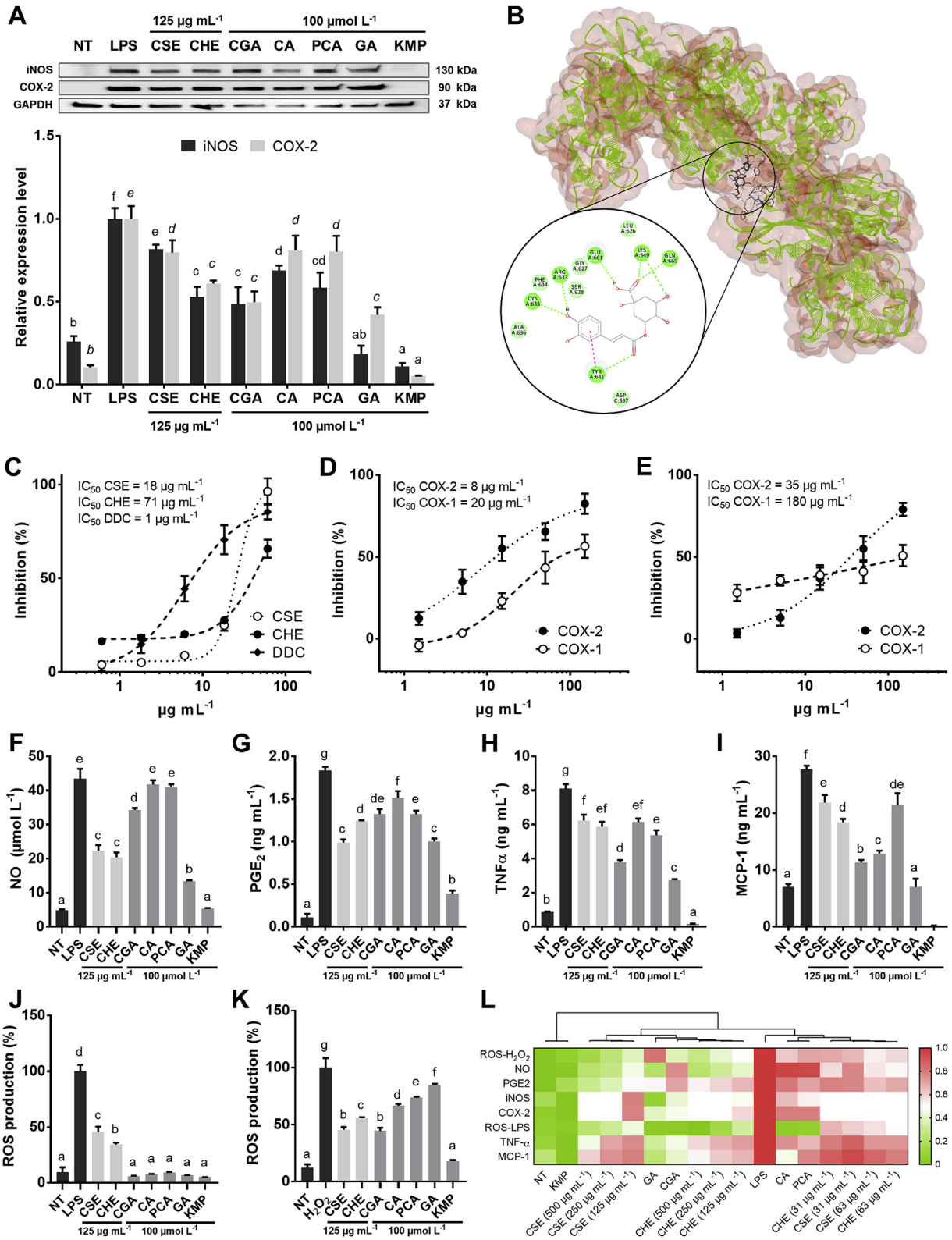

Fig. 2. Inhibitory effect of coffee silverskin (CSE) and coffee husk (CHE) aqueous extracts (125 μg mL^{-1}) and pure compounds (100 μmol L^{-1}) on the LPS-activation (1 μg mL^{-1}) of RAW264.7-Mφ. Relative expression of iNOS and COX-2 (**A**), *in silico* interaction of CGA with the catalytic site of iNOS reductase domain (**B**), inhibition of iNOS (**C**) and COX-2 (**D, E**). Production of NO (**F**), PGE_2 (**G**), TNF-α (**H**), and MCP-1(**I**), ROS upon the stimulation with LPS (**J**) and H_2O_2 (**K**). Hierarchical cluster analysis and heat map (**L**). Bars with different letters significantly differ according to ANOVA and Tukey's multiple range test ($p < 0.05$). DDC: Diphenyleneiodonium chloride; NT: non-treated cells; CGA: chlorogenic acid; CA: caffeic acid: PCA: protocatechuic acid; GA: gallic acid; KMP: kaempferol.

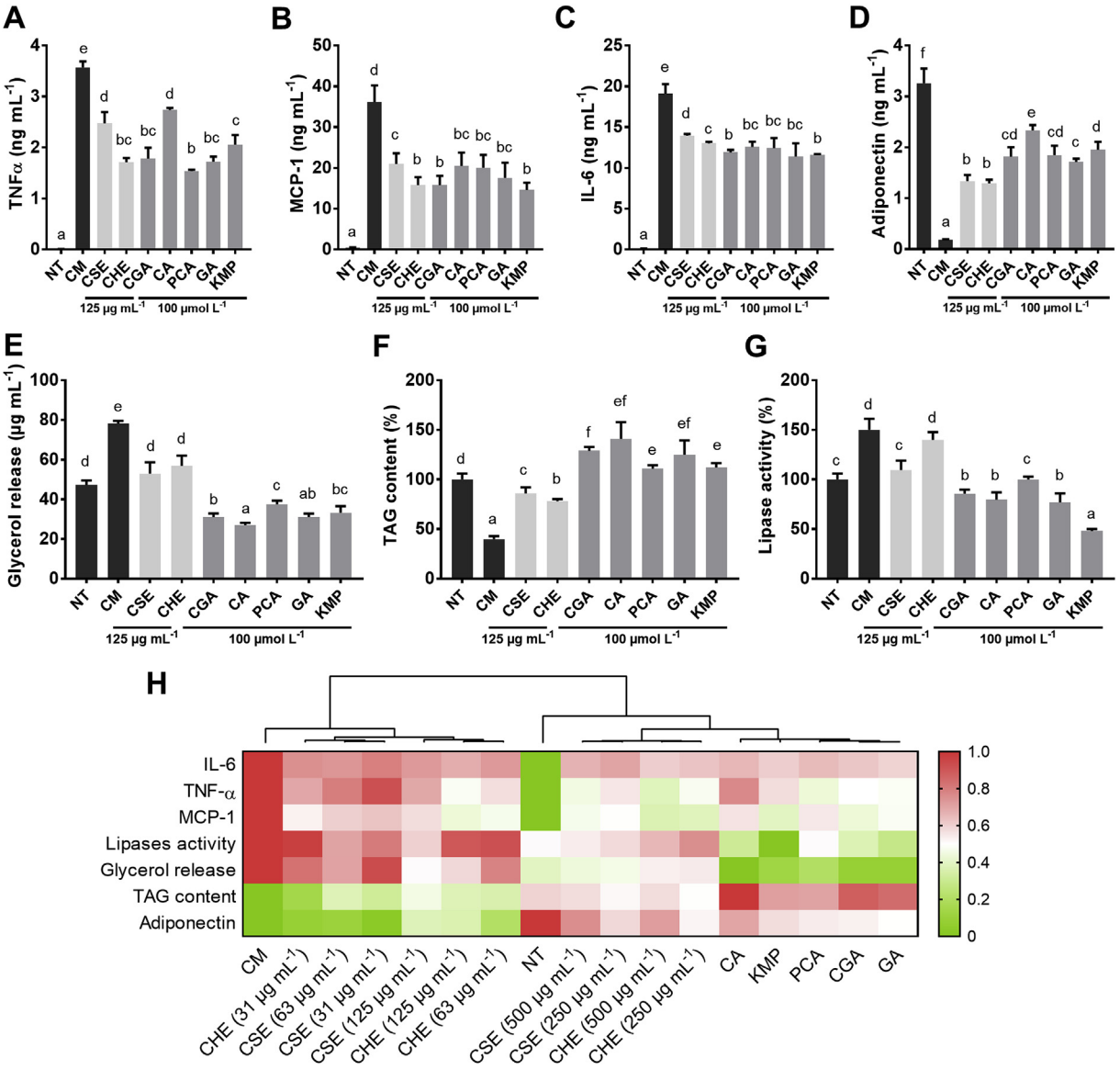

Fig. 3. Effect of coffee silverskin (CSE) and coffee husk (CHE) aqueous extracts (125 μg mL^{-1}) and pure compounds (100 μmol L^{-1}) on the release of adipokines and on inflammation-induced lipolysis in adipocytes treated with macrophage-conditioned media (CM) for 24 h: TNF-α **(A)**, MCP-1 **(B)**, IL-6 **(C)**, adiponectin **(D)**, glycerol release **(E)**, intracellular triglycerides content **(F)**, and lipase activity **(G)**. Hierarchical cluster analysis and heat map (**H**). The results are expressed as mean ± SD. Bars with different letters significantly ($p < 0.05$) differ according to ANOVA and Tukey's multiple range test. NT: non-treated cells; CGA: chlorogenic acid; CA: caffeic acid: PCA: protocatechuic acid; GA: gallic acid; KMP: kaempferol.

and CHE while IRS-1 serine phosphorylation diminished; CSE decreased the phosphorylation of 5 residues (Ser307, -2.9; Ser636, −1.8; Ser639, −4.7; Ser794, −2.4; Ser1101, −1.4) and CHE of 6 (Ser307, −1.9; Ser312, −1.4; Ser323, −1.4; Ser636, −1.3; Ser639, −4.6; Ser794, −1.7). CSE and CHE induce AKT activity by the up-phosphorylation of 7 and 6 residues, respectively. PI3K was phosphorylated and activated only by CSE. CHE inhibited phosphatase and tensin homolog (PTEN) by increasing its phosphorylation to a greater extent and more residues than CSE. CSE and CHE modulated the phosphorylation of 4 different MAPKs. Coffee by-products extracts also reduced IKK phosphorylation. The activity of AMP-activated protein kinase (AMPK) and liver kinase B1 (LKB1) was also regulated. Protein kinase C (PKC) θ phosphorylation was reduced by CSE (Thr538, −3.1; Ser676, −1.4) and by CHE (Thr538, −4.8; Ser676, −1.3) while PKC ζ was phosphorylated only by CHE (Thr410, 1.6; T560, 1.6), reducing and enhancing their activities, respectively. In addition, coffee phenolic interacted *in silico* with phosphatases, which could reduce insulin action, suggesting their potential inhibition (Supplementary Table 3).

Adipocytes treated with the inflammatory factors from Mφ-CM did not translocate GLUT4 into the cell membrane (Fig. 5A and B). Nevertheless, the co-treatment with extracts and pure compounds inhibited CM action, being also CGA and PCA the compounds showing the best protective effects. Insulin-dependent glucose uptake was therefore inhibited ($p < 0.05$) by the treatment of adipocytes with Mφ-CM (Fig. 5C). However, CSE and CHE treatments increased insulin-dependent glucose uptake (36 and 45%, respectively). The regulative effect of the pure phenolic compounds, primarily CGA and PCA, was significantly higher ($p < 0.05$), enhancing glucose uptake.

3.6. Protein network, KEGG, and multivariate analyses identified insulin and PI3K-AKT as key signaling pathways and kaempferol as the most active compound

CSE and CHE treatments were involved in the regulation of the expression/phosphorylation of 68 and 80 protein, respectively, sharing effects in 49 of them (Fig. 6A). Biological processes affected by

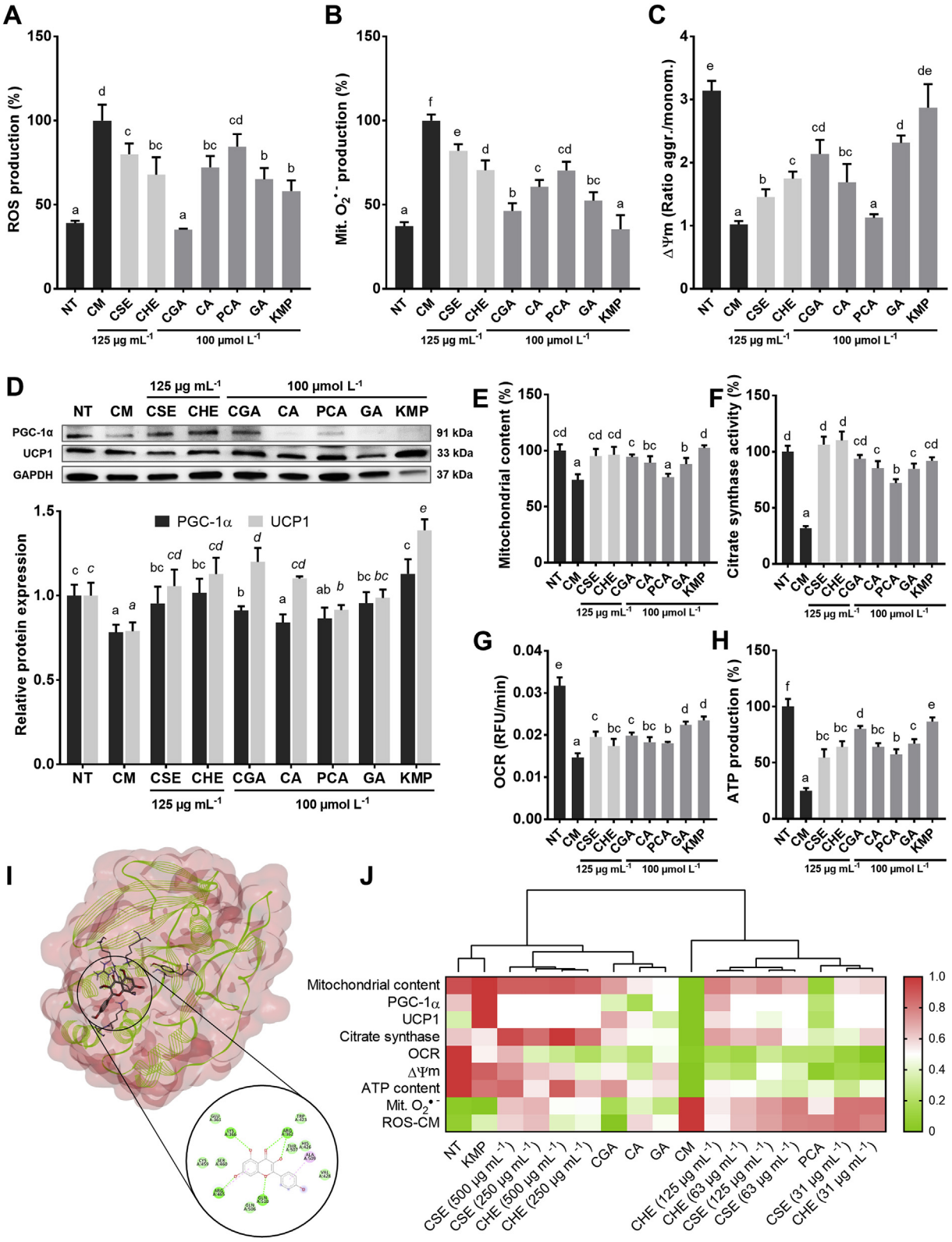

Fig. 4. Modulation of mitochondrial function of coffee silverskin (CSE) and coffee husk (CHE) aqueous extracts (125 μg mL^{-1}) and pure compounds (100 μmol L^{-1}) in 3T3-L1 adipocytes treated with macrophage-conditioned media (CM) for 24 h. Production of intracellular reactive oxygen species (ROS) (**A**), superoxide radical (**B**), mitochondrial membrane potential (ΔΨm) **(C)**, relative protein expression of PGC-1α and UCP1 (**D**), mitochondrial content (**E**), citrate synthase activity (**F**), oxygen consumption rate (OCR) (**G**), and ATP production (**H**). *In silico* interaction of KMP with the catalytic site of SHP-2 (**I**). Hierarchical cluster analysis and heat map (**J**). The results are expressed as mean ± SD. Bars with different letters significantly ($p < 0.05$) differ according to ANOVA and Tukey's multiple range test. NT: non-treated cells; CGA: chlorogenic acid; CA: caffeic acid: PCA: protocatechuic acid; GA: gallic acid; KMP: kaempferol.

Table 1
Differential phosphorylated/non-phosphorylated ratio ($p < 0.05$) of proteins related to the insulin pathway of insulin-resistant 3T3-L1 cells in response to treatment with phenolic extracts from coffee silverskin and husk. Protein full names and biological functions are found in Supplementary Table 4.

Protein code (Phosphorylation)	Effect of phosphorylation	Phosphorylated/Non-phosphorylated ratio[1]			Fold change	
		CM	CSE	CHE	CSE/CM	CHE/CM
Insulin receptor signaling						
INSR (Y1361)	Induces activity	5.5	8.6	23.1	**1.6**	**4.2**
INSR (Y1355)	Induces activity	1.0	2.4	1.4	**2.4**	**1.4**
IRS-1 (S307)	Inhibits molecular association	2.2	0.8	1.2	**–2.9**	**–1.9**
IRS-1 (S312)	Inhibits molecular association	2.0	1.7	1.4	-	**–1.4**
IRS-1 (S323)	Inhibits activity	0.2	0.2	0.1	-	**–1.4**
IRS-1 (S636)	Inhibits molecular association	2.3	1.3	1.7	**–1.8**	**–1.3**
IRS-1 (S639)	Inhibits molecular association	0.6	0.1	0.1	**–4.7**	**–4.6**
IRS-1 (S794)	Inhibits molecular association	1.8	0.8	1.1	**–2.4**	**–1.7**
IRS-1 (S1101)	Inhibits activity	0.0	0.0	0.0	**–1.4**	-
Gab1 (Y627)	Induces molecular association	1.2	2.5	3.4	**2.1**	**2.9**
Gab1 (Y659)	Induces molecular association	0.7	1.0	0.7	**1.4**	-
GAB2 (S159)	Inhibits molecular association	1.4	1.3	2.1	-	**1.5**
PI3K-AKT-PKB signaling						
4E-BP1 (T45)	Inhibits molecular association	1.5	0.9	0.7	**–1.7**	**–2.2**
4E-BP1 (S65)	Inhibits molecular association	0.0	0.0	0.0	-	**–1.9**
4E-BP1 (T70)	Inhibits activity/molecular association	0.7	0.2	0.6	**–3.6**	-
AKT (T308)	Induces activity	0.3	0.4	0.7	**1.3**	**2.4**
AKT (Y326)	Induces activity	0.4	0.5	0.5	-	**1.3**
AKT (S473)	Induces activity	1.2	1.7	1.5	**1.5**	**1.3**
AKT1 (S124)	Induces activity	0.7	1.9	1.9	**2.6**	**2.6**
AKT1 (S246)	Induces activity	0.8	1.7	1.0	**2.0**	-
AKT1 (Y474)	Induces activity	1.3	2.1	1.8	**1.6**	**1.4**
AKT1 (T72)	Induces activity	1.9	2.8	4.9	**1.5**	**2.6**
AKT2 (S474)	Induces activity	4.3	7.8	4.9	**1.8**	-
eIF2a (S51)	Inhibits activity	0.2	0.2	0.2	**–1.6**	-
eIF4E (S209)	Inhibits molecular interaction	2.2	0.8	1.6	**–2.9**	**–1.3**
eIF4G (S1108)	Inhibits activity	0.2	0.1	0.1	**–1.2**	**–1.6**
FKHR (S256)	Inhibits molecular association	0.8	2.2	1.1	**2.7**	**1.3**
FKHR (S319)	Inhibits molecular association	1.3	2.2	1.9	**1.7**	**1.4**
FKHRL1 (S253)	Inhibits activity	0.7	1.1	1.2	**1.5**	**1.7**
FOXO1A (S329)	Inhibits activity	0.9	1.1	1.4	-	**1.5**
GSK3 α (S21)	Inhibits activity	1.2	0.8	1.1	**–1.4**	-
GSK3 α/β (Y216/279)	Induces activity	2.0	0.8	1.9	**–2.5**	-
GSK3 β(S9)	Inhibits activity	3.9	2.1	2.5	**–1.8**	**–1.6**
HSL (S552/563)	Induces activity	0.3	0.2	0.1	-	**–2.1**
HSL (S554)	Inhibits activity	0.8	1.8	1.0	**2.2**	-
mTOR (S2448)	Induces activity	1.8	1.6	1.1	-	**–1.7**
p70S6K (T229)	Induces activity	0.5	0.5	0.4	-	**–1.3**
p70S6K (S371)	Induces activity	1.4	0.9	1.2	**–1.5**	-
p70S6K (S411)	Induces activity	1.0	1.0	1.3	-	**1.3**
p70S6K (S418)	Induces activity	1.5	4.0	1.4	**2.7**	-
p70S6K (T421)	Induces activity	1.6	0.3	0.4	**–4.9**	**–4.4**
p70S6K (S424)	Induces activity	1.9	0.7	1.0	**–2.7**	**–1.9**
p70S6K β (S423)	Induces activity	1.6	2.1	2.7	**1.4**	**1.7**
PI3K α/γ (Y467/Y199)	Induces activity	0.9	2.5	1.0	**2.7**	-
PI3K α (Y607)	Induces activity	0.0	0.0	0.0	**1.5**	-
PTEN (S370)	Inhibits activity	0.1	0.1	1.0	-	**8.0**
PTEN (S380)	Inhibits activity	0.0	0.1	0.1	**2.9**	**3.2**
PTEN (S380/T382/T383)	Inhibits activity	0.2	0.2	1.9	-	**10.1**
MAPK signaling						
c-Raf (S296)	Inhibits activity	0.1	0.1	0.2	-	**2.2**
c-Raf (S43)	Inhibits activity	0.1	0.1	0.1	**1.5**	**1.3**
CrkII/p38 (Y221)	Inhibits activity	0.0	0.1	0.3	**1.5**	**6.6**
ERK1 (T202)	Induces activity	3.1	1.3	2.8	**–2.3**	-
ERK1 (Y204)	Induces activity	2.0	1.3	1.5	**–1.6**	**–1.3**
ERK3 (S189)	Induces molecular association	1.5	1.7	2.5	-	**1.7**
MEK1 (S217)	Induces activity	1.3	0.5	0.8	**–2.5**	**–1.6**
MEK1 (S221)	Induces activity	3.6	2.6	3.1	**–1.4**	-
MEK1 (T286)	Inhibits activity	0.0	0.0	0.0	-	**1.5**
MEK1 (T291)	Inhibits activity	0.7	0.8	1.3	-	**1.9**
MEK1 (S298)	Induces activity	0.1	0.1	0.0	-	**–3.0**
MEK2 (T394)	Inhibits activity	1.6	2.2	2.9	**1.4**	**1.8**
IKK-NF-κB signaling						
IKK α (T23)	Induces activity	1.0	0.6	1.0	**–1.6**	-
IKK α/β (S180/181)	Induces activity	0.4	0.3	0.2	-	**–2.6**
IKK β (Y199)	Induces activity	0.0	0.0	0.0	**–2.0**	**–3.5**
IKK γ (S31)	Induces transcription	0.0	0.0	0.0	**–1.6**	-
IKK γ(S85)	Induces activity	0.3	0.3	0.1	-	**–2.5**
iNOS (expression)		0.1	0.1	0.1	-	**–1.7**
Other signaling cascades						

(*continued on next page*)

Table 1 (*continued*)

Protein code (Phosphorylation)	Effect of phosphorylation	Phosphorylated/Non-phosphorylated ratio[1]			Fold change	
		CM	CSE	CHE	CSE/CM	CHE/CM
AMPK α1 (T174)	Induces activity	1.8	0.6	1.0	**–2.8**	**–1.9**
AMPK α1/2 (S485/491)	Inhibits activity	2.3	4.1	4.8	**1.8**	**2.1**
AMPK β1 (S182)	Regulates cellular localization	0.4	0.4	0.2	-	**–1.7**
ACLY (S454)	Induces activity	0.3	0.2	0.2	-	**–1.4**
BAD (S112)	Inhibits molecular association	0.9	0.9	1.5	-	**1.7**
BAD (S134)	Inhibits molecular association	0.7	0.8	0.9	-	**1.4**
BAD (S136)	Inhibits molecular association	1.0	1.4	2.0	**1.4**	**2.0**
BAD (S155)	Inhibits molecular association	1.8	3.0	2.4	**1.7**	**1.3**
BAD (S91/128)	Inhibits molecular association	0.7	0.8	2.0	-	**2.7**
CAV1 (Y14)	Induces activity	1.7	3.2	3.6	**1.9**	**2.1**
LKB1 (T189)	Inhibits activity	1.6	1.2	0.5	**–1.4**	**–3.3**
LKB1 (S428)	Induces activity	2.0	2.4	3.0	-	**1.5**
PKA CAT (T197)	Induces activity	0.6	1.2	0.7	**1.9**	-
PKC pan activation site	Induces activity	0.9	0.7	0.5	**–1.3**	**–1.6**
PKC θ (T538)	Induces activity	0.0	0.0	0.0	**–3.1**	**–4.8**
PKC θ (S676)	Induces activity	1.7	1.2	1.3	**–1.4**	**–1.3**
PKC ζ (T410)	Induces activity	0.7	0.8	1.0	-	**1.6**
PKC ζ (T560)	Induces activity	1.0	1.1	1.6	-	**1.6**
PP1α (T320)	Inhibits activity	0.2	1.3	3.1	**6.1**	**14.8**
PP2A-a (Y307)	Inhibits activity	0.0	0.0	0.1	**2.3**	**13.2**
Ras-GRF1 (S916)	Induces activity	0.2	0.2	0.2	-	**1.4**
Shc (Y349)	Induces activity	0.1	0.1	0.2	-	**1.8**
Shc (Y427)	Induces activity	0.7	1.1	1.0	**1.5**	**1.4**
SHP-2 (Y542)	Induces molecular association	1.4	1.0	0.4	**–1.3**	**–3.1**
SHP-2 (Y580)	Induces molecular association	1.8	1.3	1.7	**–1.4**	-
TNFR 1 (expression)		0.0	0.0	0.0	**–1.9**	**–2.2**
TSC2 (S939)	Inhibits activity	0.6	0.1	0.2	**–4.3**	**–3.3**

[1] CM, macrophages conditioned media; CHE, coffee husk aqueous phenolic extract; CSE, coffee silverskin aqueous phenolic extract.

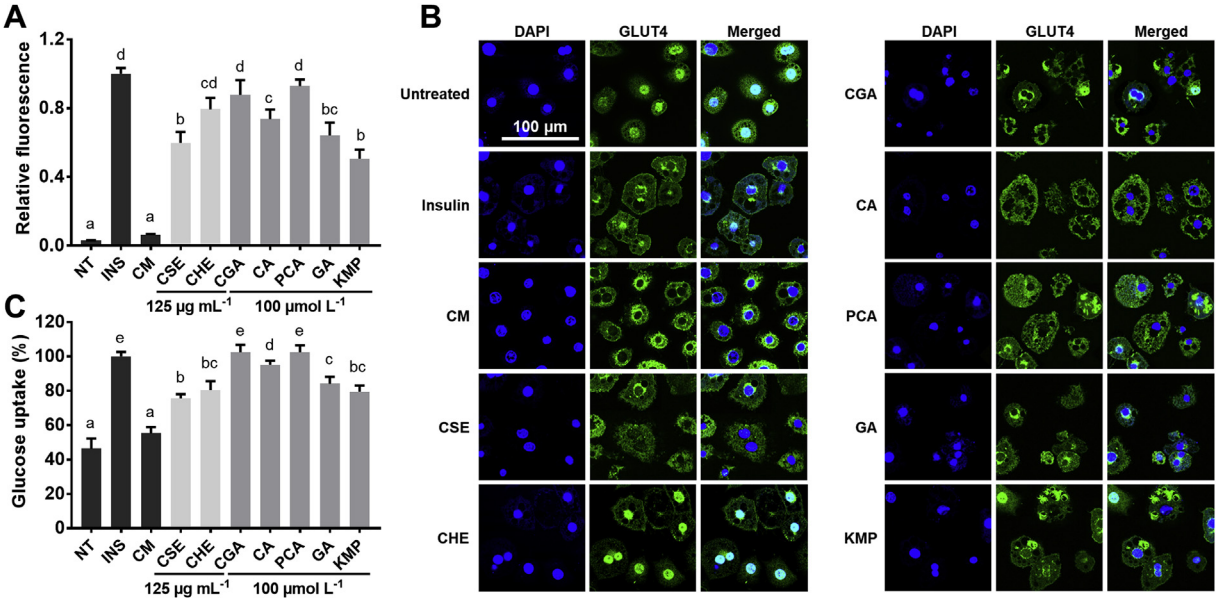

Fig. 5. Potential of coffee silverskin (CSE) and coffee husk (CHE) aqueous extracts (125 µg mL^{-1}) and pure compounds (100 µmol L^{-1}) on insulin resistance in 3T3-phL1 adipocytes treated with macrophage-conditioned media (CM) for 24 h. GLUT4 translocation into the cell membrane measured as the relative fluorescence intensity between GLUT4 and the nucleus (DAPI) (**A**), confocal laser scanning microscopy representative images (**B**), and glucose uptake (**C**), The results are expressed as mean ± SD. Bars with different letters significantly ($p < 0.05$) differ according to ANOVA and Tukey's multiple range test. NT: non-treated cells; INS: insulin-stimulated cells; CGA: chlorogenic acid; CA: caffeic acid: PCA: protocatechuic acid; GA: gallic acid; KMP: kaempferol.

treatments include regulation of phosphorylation, signal transduction, response to cytokine, regulation of NF-κB signaling and MAPK cascade (extracellular signal-regulated kinase (ERK) 1/2 and JNK cascades), and response to insulin. Among the modified proteins, most of them were implicated in insulin, PI3K-AKT, and mTOR pathways in CSE (Fig. 6 B and C) and CHE (Fig. 6D and E) treatments. Inflammation-related pathways, as Ras, chemokine, MAPK, and TNF signaling pathways were also regulated. Likewise, AMPK, cAMP, and thermogenic-related proteins were also suggested as the key pathways modified by CSE and CHE in CM-treated adipocytes. Hierarchical cluster analysis (Fig. 6F) highlighted the effect of kaempferol, which almost reverted the adverse effects produced by pro-inflammatory factors in Mφ and adipocytes. The effects of CSE and CHE (125–500 µg mL^{-1}) were comparable to those of CGA, CA, PCA, and GA (100 µmol L^{-1}).

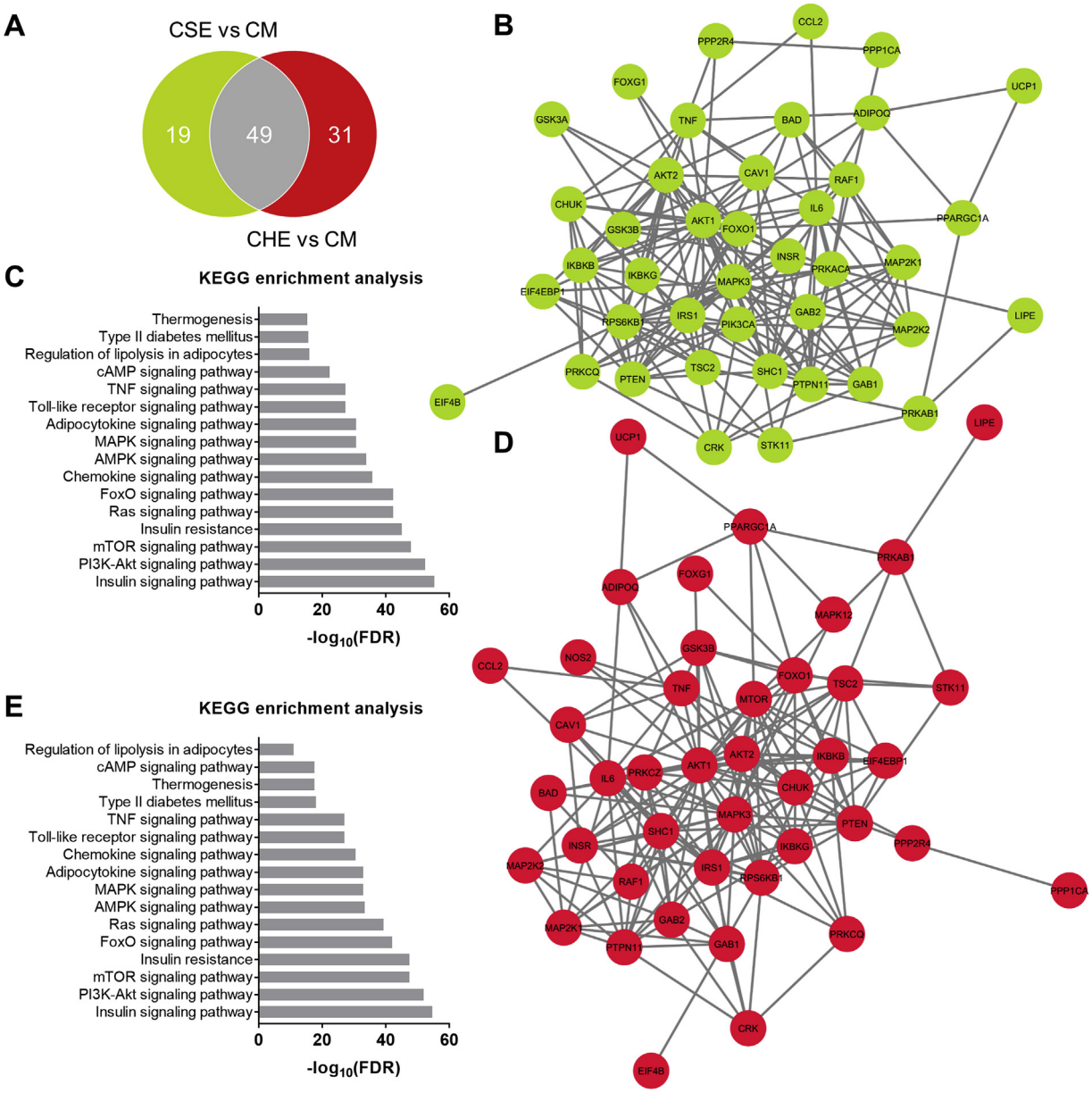

(caption on next page)

Fig. 6. Venn diagram illustrating the overlap of differentially expressed/phosphorylated protein in adipocytes by coffee silverskin (CSE) and coffee husk (CHE) aqueous phenolic extracts (**A**), protein-protein interaction networks built with STRING from the differentially expressed/phosphorylated protein in adipocytes by CSE (**B**) and CHE (**D**). KEGG pathways associated with the differentially expressed/phosphorylated proteins (**C, E**). Proteins included in the analysis were those differentially expressed in 3T3-L1 adipocytes upon CM-stimulation for the inflammation, mitochondrial function, and insulin resistance studies. Hierarchical cluster analysis and heat map (**F**) showing the modulatory effects of CSE and CHE (31–500 μg mL^{-1}) and pure compounds (100 μmol L^{-1}) on the different studied parameters of adipocytes differentiation, macrophages activation, adipocytes inflammation, mitochondrial dysfunction, and insulin resistance.

4. Discussion

The global obesity epidemic is accompanied by increasing prevalence of associated metabolic disorders (Reilly and Saltiel, 2017). Here we present, for the first time, the impact of two well-characterized phenolic-rich extracts from coffee by-products and five pure phenolic compounds composing them on *in vitro* model of obesity-related inflammation and the consequent mitochondrial dysfunction and IR. Diminishing adipocyte differentiation and increasing energy expenditure by modulating AT activity could be an attractive target for preventing obesity. In this sense, our results demonstrated that CSE and CHE not only inhibited 3T3-L1 differentiation but also increased adipocyte lipid metabolism, inducing lipolysis through the regulation of lipases. Moreover, CSE, CHE, and their main composing phenolics were able to induce a beige differentiation or "browning" of adipocytes, a process characterized by a higher mitochondrial density, activity, and increased energy expenditure (Cedikova et al., 2016). Treatments elicited an increase in mitochondrial content and aerobic CS activity. Obesity development depends not only on the balance between food intake and energy expenditure but also on the balance between white AT, as the primary energy reservoir, and brown/beige AT specialized in energy expenditure (Gómez-Hernández et al., 2016). Dietary bioactive compounds (e.g., quercetin, resveratrol, or curcumin) have demonstrated the ability to induce this phenotype in the AT and to inhibit adipogenesis (Beaudoin et al., 2013; Kobori et al., 2016; Wang et al., 2015). From our understanding, no studies have reported the mechanism and effects of the studied coffee by-products phenolics, except GA (Doan et al., 2015). Besides the effects of phenolics, caffeine could also have been exerting beneficial effects on adipogenesis and insulin resistance. Literature have demonstrated the potential effects of caffeine in reducing adipocytes differentiation, also triggering adipocyte browning (Kim et al., 2016; Yoneshiro et al., 2017).

AT is recognized as a primary contributor in the development of IR in obesity (Lorenzo et al., 2008). In hypertrophic AT, adipocytes and Mφ crosstalk to induce a chronic low-grade state of inflammation and IR resulting in increased FFAs release, oxidative stress, and chemokine/cytokine secretion, further promoting Mφ infiltration in the AT (Xu et al., 2013). Phenolic compounds present in CSE and CHE successfully mitigated inflammatory processes in LPS-stimulated Mφ, inhibiting the expression and activity of iNOS and COX-2 and the production of their reaction products, NO and PGE_2. Additionally, CSE and CHE phenolics were able to diminish the production of inflammatory cytokines that lead to the inflammatory paracrine loop in the AT, TNF-α, and MCP-1. In 3T3-L1 adipocytes stimulated with RAW264.7-CM, CSE, CHE, and their phenolics inhibited the secretion of TNF-α, MCP-1, and IL-6. These cytokines increase the adipose triglyceride lipase and hormone-sensitive lipase (HSL) activity, which increases FFAs release, generating a vicious cycle (Langin, 2006). Phenolic compounds from CSE and CHE were able to reduce the extent of this lipolysis by regulating adipocyte lipases activity, hence maintaining the content of TAG. Likewise, HSL activity was inhibited by dephosphorylating Ser552 and phosphorylating Ser554 residues. These evidences support the ability of coffee by-products extracts to break the inflammatory loop Mφ-adipocytes, via not only reducing Mφ and adipocyte inflammatory factors secretion but also decreasing the release of FFAs that may activate Mφ (Olefsky and Glass, 2010). Phenolics may induce lipolysis in basal conditions through the activation of HSL while inhibit lipolysis in inflammatory conditions through the downregulation of perilipins via inactivation of ERK1/2, JNK, and NF-κB (Langin, 2006; Yang et al., 2011). Likewise, phenolic may be inhibiting the elevated activity of adipose triglyceride lipase (ATGL), the rate-limiting enzyme catalyzing triglyceride hydrolysis, that has been shown to improve inflammation in mice fed with a high fat diet (Schoiswohl et al., 2015). Although this is still controversial, previous studies revealed similar results when treating adipocytes with anthocyanins (Luna-Vital et al., 2017). Coffee by-products demonstrated ability, along with CGA and CA, to inhibit inflammation by decreasing IL-8 release in gastric epithelial and intestinal cells *in vitro* (Magoni et al., 2018; Shin et al., 2015). In addition, CGA has proved to inhibit inflammation in Mφ reducing the secretion of pro-inflammatory factors via attenuating the activation of NF-κB and JNK pathways (Hwang et al., 2014; Shan et al., 2009). Here, CSE and CHE suppressed adipocyte inflammatory status by regulating NF-κB and MAPK pathways, including ERK, JNK, and p38. These signal transduction pathways were hindered by CSE and CHE through the inhibition of the activity of mitogen-activated protein kinase kinase (MEK) 1/2, adapter molecule crk (CrkII/p38), RAF proto-oncogene serine/threonine-protein kinase (c-Raf), and protein kinase C (PKC) θ, through the modulation of their phosphorylation pattern. Moreover, results proposed that treatments arrested toll-like receptor 4 (TLR4) signaling, responsible in part of the here-detailed pro-inflammatory responses. Inhibition of TLR4 activation could be an approach to handle obesity-induced inflammation and IR (Schäffler and Schölmerich, 2010).

Several studies have demonstrated the role of mitochondria in obesity and IR (Bhatti et al., 2017; Rector et al., 2010). It has been seen that ROS and TNF-α promote mitochondrial dysfunction in adipocytes (Chen et al., 2010). In this study, coffee by-products aqueous extracts and pure compounds suppressed the intensified production of ROS and recovered the ΔΨm. Elevated oxidative stress and inflammation may create a vicious cycle that ultimately accelerates obesity-related IR and the loss of mitochondrial function. Mitochondrial dysfunction is linked with oxidative stress being an important source of ROS but also a major target for them (Bhatti et al., 2017). Hence, the phenolic compounds from CSE and CHE promoted mitochondrial biogenesis and preserved its function under inflammatory conditions through the activation of PGC-1α, a transcriptional coactivator that is the central inducer of these processes (Austin and St-Pierre, 2012). TNF-α suppresses UCP1 expression promoter via ERK1/2 activation (Sakamoto et al., 2013); CSE, CHE abrogated this effect. Coffee by-products extracts decreased ERK1 activity by the reduction of Thr202 and Tyr204 phosphorylation. Likewise, MEK1/2 activity, which activates ERK1/2, was also inhibited by the modulation of several phosphorylation sites. CGA has shown protective effects on mitochondria, scavenging ROS and alleviating mitochondrial damage, and suppressing inflammation processes (Hwang et al., 2014; Shan et al., 2009). KMP can reverse the phosphorylation of ERK1/2, p38, and JNK, and the activation of NF-κB (Yoon et al., 2013), as well as protect mitochondria against ROS (Lagoa et al., 2011), thus, preserving mitochondrial function. Nutritional interventions improving mitochondrial biogenesis, dynamics, bioenergetics, and oxidative stress are proposed as effective tools in the prevention of IR and metabolic syndrome.

IR is strongly associated with the pathogenesis of T2D and obesity and results from a sustained low-grade inflammatory status and the loss of the mitochondrial function (Ye, 2013). IR may be arrested using dietary bioactive compounds including anti-inflammatory phytochemicals present in coffee by-products. CSE and CHE differently modulated the phosphorylation pattern of the insulin-signaling pathway, therefore,

hindering IR. Upon insulin interaction with its receptor (INSR), tyrosine phosphorylation activates IRS-1, which further initiate PI3K/AKT signaling, responsible for GLUT4 translocation and glucose uptake. TNF-α, among other pro-inflammatory stimuli, produces AT-IR via the induction of serine phosphorylation, and inactivation, of IRS-1 through the activity NF-κB, ERK, JNK, mammalian target of rapamycin (mTOR), and PKC θ (Copps and White, 2012). CSE and CHE activated PI3K/AKT signal transduction via increasing INSR tyrosine phosphorylation and decreasing IRS-1 serine phosphorylation. Besides, the inhibition of the activity of phosphatases (PTEN and SHP-2), both by modulation of their phosphorylation and by direct docking, prevented PI3K and IRS-1 inactivation. PKC ζ and AMPK signaling were as well stimulated, via activation of PI3K and LKB1 activities, respectively. CSE and CHE suppressed mTOR and ribosomal protein S6 kinase (p70S6K) activity mediated by tuberous sclerosis protein 2 (TSC2) dephosphorylation and activation. Evidence indicated that JNK evokes mTOR and p70S6K activity, resulting in INS-1 serine phosphorylation. CSE- and CHE-mediated reduction of inflammatory processes also reverses inflammation-triggered mitochondrial dysfunction and IR (Ardestani and Maedler, 2018). Thus, the orchestrated regulation of insulin signaling motivated GLUT4 translocation as the subsequent glucose uptake. Not only CSE and CHE but also their phenolic compounds were able to maintain insulin-dependent glucose uptake by the stimulation of GLUT4 translocation. CGA, the main component of both extracts exhibited significant protective effects against inflammation-derived IR, suggesting its major contribution to the effects of the extracts. CA and PCA similarly exerted positive effects. CGA proved insulin-sensitizing activity activating glucose uptake through AKT and AMPK pathways in hepatocytes and skeletal muscle cells (Gao et al., 2018; Ong et al., 2012). CA revealed protective effects against TNF-α-induced hepatic insulin resistance, increasing glucose uptake via INSR and PI3K activation (Huang et al., 2009). PCA demonstrated to exert insulin-mimicking activity eliciting INSR signaling, reversing of INS-1 serine phosphorylation, and activating PI3K/AKT and AMPK signaling pathways, therefore favoring GLUT4 translocation and glucose uptake (Scazzocchio et al., 2015). However, one of the potential limitations of this work is the low bioavailability of pure phenolic compounds, which may not reach the adipose tissue, due to microbial and phase II metabolism. Chlorogenic acid and other compounds found in CSE and CHE may be metabolized and found in concentrations ranging in the μmol L^{-1} level (Lang et al., 2013; Nardini et al., 2002).

5. Conclusions

In summary, coffee by-products aqueous extracts, CSE and CHE, and their major phenolics attenuated inflammation derived from Mφ-adipocytes interaction. Additionally, IR and mitochondrial dysfunction were prevented via modulation of the insulin/PI3K-AKT, NF-κB/MAPK and AMPK pathways (Fig. 7). We demonstrated, for the first time, that the phenolic compounds composing aqueous phenolic-rich extracts from coffee silverskin and coffee husk alleviated the complications of adipogenesis and inflammation *in vitro*. Our study presents a mechanistic evaluation of the inhibitory effects of CSE, CHE and their main phenolics, CGA, CA, PCA, GA, and KMP, using RAW264.7-Mφ and 3T3-L1 adipocytes. Taken together, our results support the notion that phenolic compounds from coffee by-products can trigger a reduction in adipogenesis and induce browning in adipocytes and that the attenuation of the paracrine interplay Mφ-adipocytes can prevent the consequent effects on the loss of mitochondrial function and insulin sensitivity. This study presents novel insights into the use of coffee by-products as sustainable food ingredients to encounter obesity and inflammation-related disorders. Furthermore, we provide new knowledge on the underlying mechanism of action of phenolic compounds composing coffee silverskin and coffee husk. Future animal and clinical investigations will be necessary to confirm the effects observed *in vitro* and determine the absorption and metabolism of coffee silverskin and husk phenolic compounds and their beneficial and potentially harmful effects. In conclusion, our results proved that phenolic compounds from coffee by-products could induce positive effects on adipogenesis and its inflammatory-related complications, mitochondrial dysfunction, and insulin resistance.

Authors contributions

M.R.H., Y.A., M.A.M.C., and E.D.M. proposed the project; M.R.H. and E.D.M. conceived and designed the analysis; M.R.H. and Q.Z. performed the analysis; M.R.H. developed and wrote the article; Y.A., M.A.M.C., and E.D.M. provided scientific guidance throughout the research and revised and edited the manuscript. All authors read and approved the final version of the manuscript.

Conflicts of interest

The authors declare no conflict of interest.

Declaration of interests

The authors declare that they have no known competing financial interests or personal relationships that could have appeared to influence the work reported in this paper.

Acknowledgments

This study was funded by the Ministry of Economy and Competitiveness, SUSCOFFEE project (AGL2014-57239-R), and the USDA-NIFA-HATCH (project 1014457). M. Rebollo-Hernanz thanks the FPU program of the Ministry of Science, Innovation, and Universities for his predoctoral fellowship (FPU15/04238) and the support for the international research stay (EST17/00823).

Abbreviations

ΔΨm	mitochondrial membrane potential
AKT	protein kinase B
AMPK	AMP-activated protein kinase
AT	adipose tissue
ATP	adenosine triphosphate
CA	caffeic acid
CGA	chlorogenic acid
CHE	coffee husk aqueous phenolic extract
CM	macrophages conditioned media
COX	cyclooxygenase
CS	citrate synthase
CSE	coffee silverskin aqueous phenolic extract
ERK	extracellular signal-regulated kinase
GA	gallic acid
GLUT4	glucose transporter type 4
IKK	inhibitor of kappa B kinase
iNOS	inducible nitric oxide synthase
INSR	insulin receptor
IR	insulin resistance
IRS-1	insulin receptor substrate 1
JNK	Jun N-terminal kinase
KMP	kaempferol
LKB1	liver kinase B1
MCP-1	monocyte chemoattractant protein 1
mTOR	mammalian target of rapamycin
Mφ	macrophages
NF-κB	nuclear factor kappa-light-chain-enhancer of activated B cells
OCR	oxygen consumption rate
p70S6K	ribosomal protein S6 kinase
PCA	protocatechuic acid

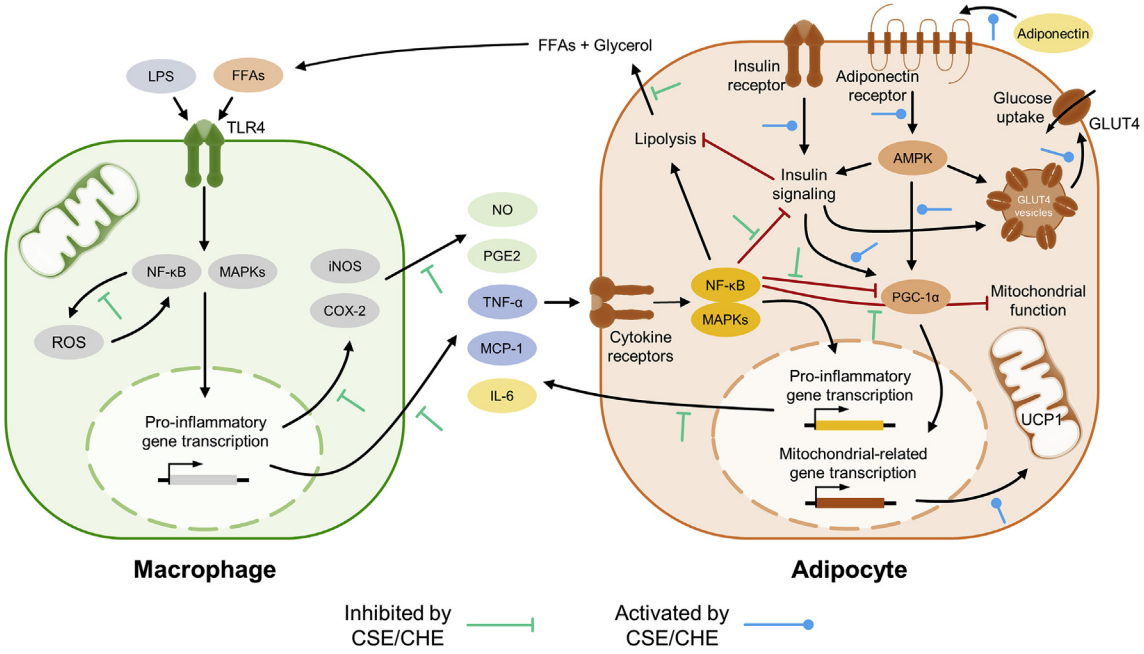

Fig. 7. Integrative diagram illustrating the underlying molecular mechanism of the inhibitory effect of CSE and CHE on obesity-related inflammation, insulin resistance, and mitochondrial dysfunction in a model of inflammation between macrophages an adipocytes.

PDK-1	phosphoinositide-dependent protein kinase-1
PGC-1α	peroxisome proliferator-activated receptor γ coactivator 1-α
PGE_2	prostaglandin E2
PI3K	phosphoinositide 3-kinase
PKC	protein kinase C
PTEN	phosphatase and tensin homolog
PTP1B	protein tyrosine phosphatase-1B
ROS	reactive oxygen species
SHP-2	protein-tyrosine phosphatase 1D
T2D	type 2 diabetes
TAG	triglycerides
TLR4	toll-like receptor 4
TNF-α	tumor necrosis factor alpha
UCP1	uncoupling protein 1

Appendix A. Supplementary data

Supplementary data to this article can be found online at https://doi.org/10.1016/j.fct.2019.110672.

References

Aguilera, Y., Martin-Cabrejas, M.A., González de Mejia, E., 2016. Phenolic compounds in fruits and beverages consumed as part of the Mediterranean diet: their role in prevention of chronic diseases. Phytochem. Rev. 15, 405–423. https://doi.org/10.1007/s11101-015-9443-z.

Aguilera, Y., Rebollo-Hernanz, M., Cañas, S., Taladrid, D., Martin-Cabrejas, M., 2019. Response surface methodology to optimise the heat-assisted aqueous extraction of phenolic compounds from coffee parchment and their comprehensive analysis. Food & Function. https://doi.org/10.1039/C9FO00544G.

Ardestani, A., Maedler, K., 2018. mTORC1 and IRS1: another deadly kiss. Trends Endocrinol. Metab. 29, 737–739. https://doi.org/10.1016/J.TEM.2018.07.003.

Austin, S., St-Pierre, J., 2012. PGC1 and mitochondrial metabolism - emerging concepts and relevance in ageing and neurodegenerative disorders. J. Cell Sci. 125, 4963–4971. https://doi.org/10.1242/jcs.113662.

Beaudoin, M.-S., Snook, L.A., Arkell, A.M., Simpson, J.A., Holloway, G.P., Wright, D.C., 2013. Resveratrol supplementation improves white adipose tissue function in a depot-specific manner in Zucker diabetic fatty rats. Am. J. Physiol. Integr. Comp. Physiol. 305, R542–R551. https://doi.org/10.1152/ajpregu.00200.2013.

Bhatti, J.S., Bhatti, G.K., Reddy, P.H., 2017. Mitochondrial dysfunction and oxidative stress in metabolic disorders - a step towards mitochondria based therapeutic strategies. Biochim. Biophys. Acta (BBA) - Mol. Basis Dis. 1863, 1066–1077. https://doi.org/10.1016/J.BBADIS.2016.11.010.

Brand, M.D., Orr, A.L., Perevoshchikova, I.V., Quinlan, C.L., 2013. The role of mitochondrial function and cellular bioenergetics in ageing and disease. Br. J. Dermatol. 169, 1–8. https://doi.org/10.1111/bjd.12208. Suppl.

Cedikova, M., Kripnerová, M., Dvorakova, J., Pitule, P., Grundmanova, M., Babuska, V., Mullerova, D., Kuncova, J., 2016. Mitochondria in white, brown, and beige adipocytes. Stem Cell. Int. 2016, 6067349. https://doi.org/10.1155/2016/6067349.

Chen, X.-H., Zhao, Y.-P., Xue, M., Ji, C.-B., Gao, C.-L., Zhu, J.-G., Qin, D.-N., Kou, C.-Z., Qin, X.-H., Tong, M.-L., Guo, X.-R., 2010. TNF-α induces mitochondrial dysfunction in 3T3-L1 adipocytes. Mol. Cell. Endocrinol. 328, 63–69. https://doi.org/10.1016/J.MCE.2010.07.005.

Copps, K.D., White, M.F., 2012. Regulation of insulin sensitivity by serine/threonine phosphorylation of insulin receptor substrate proteins IRS1 and IRS2. Diabetologia 55, 2565–2582. https://doi.org/10.1007/s00125-012-2644-8.

del Castillo, M.D., Iriondo-DeHond, A., Fernandez-Gomez, B., Martinez-Saez, N., Rebollo-Hernanz, M., Martín-Cabrejas, M.A., Farah, A., 2019. Coffee antioxidants in chronic diseases. In: Farah, A. (Ed.), Coffee: Consumption and Health Implications. Royal Society of Chemistry, Cambridge, pp. 20–56. https://doi.org/10.1039/9781788015028-00020.

Doan, K.V., Ko, C.M., Kinyua, A.W., Yang, D.J., Choi, Y.-H., Oh, I.Y., Nguyen, N.M., Ko, A., Choi, J.W., Jeong, Y., Jung, M.H., Cho, W.G., Xu, S., Park, K.S., Park, W.J., Choi, S.Y., Kim, H.S., Moh, S.H., Kim, K.W., 2015. Gallic acid regulates body weight and glucose homeostasis through AMPK activation. Endocrinology 156, 157–168. https://doi.org/10.1210/en.2014-1354.

Dorsey, B.M., Jones, M.A., 2017. Healthy components of coffee processing by-products. In: Handbook of Coffee Processing By-Products, pp. 27–62. https://doi.org/10.1016/B978-0-12-811290-8.00002-5.

Fernandez-Gomez, B., Lezama, A., Amigo-Benavent, M., Ullate, M., Herrero, M., Martín, M.Á., Mesa, M.D., del Castillo, M.D., 2016a. Insights on the health benefits of the bioactive compounds of coffee silverskin extract. J. Funct. Foods 25, 197–207. https://doi.org/10.1016/j.jff.2016.06.001.

Fernandez-Gomez, B., Ramos, S., Goya, L., Mesa, M.D., del Castillo, M.D., Martín, M.Á., 2016b. Coffee silverskin extract improves glucose-stimulated insulin secretion and protects against streptozotocin-induced damage in pancreatic INS-1E beta cells. Food Res. Int. 89, 1015–1022.

Gao, J., He, X., Ma, Y., Zhao, X., Hou, X., Hao, E., Deng, J., Bai, G., 2018. Chlorogenic acid targeting of the AKT PH domain activates AKT/GSK3β/FOXO1 signaling and improves glucose metabolism. Nutrients 10. https://doi.org/10.3390/nu10101366.

Gómez-Hernández, A., Beneit, N., Díaz-Castroverde, S., Escribano, Ó., 2016. Differential role of adipose tissues in obesity and related metabolic and vascular complications. Int. J. Endocrinol. 2016, 1–15. https://doi.org/10.1155/2016/1216783.

Huang, D.-W., Shen, S.-C., Wu, J.S.-B., 2009. Effects of caffeic acid and cinnamic acid on glucose uptake in insulin-resistant mouse hepatocytes. J. Agric. Food Chem. 57, 7687–7692. https://doi.org/10.1021/jf901376x.

Hwang, S.J., Kim, Y.-W., Park, Y., Lee, H.-J., Kim, K.-W., 2014. Anti-inflammatory effects of chlorogenic acid in lipopolysaccharide-stimulated RAW 264.7 cells. Inflamm. Res. 63, 81–90. https://doi.org/10.1007/s00011-013-0674-4.

Iriondo-DeHond, A., Aparicio García, N., Fernandez-Gomez, B., Guisantes-Batan, E., Velázquez Escobar, F., Blanch, G.P., San Andres, M.I., Sanchez-Fortun, S., del Castillo, M.D., 2018. Validation of coffee by-products as novel food ingredients. Innov. Food Sci. Emerg. Technol. https://doi.org/10.1016/J.IFSET.2018.06.010.

Iriondo-DeHond, A., Haza, A.I., Ávalos, A., del Castillo, M.D., Morales, P., 2017. Validation of coffee silverskin extract as a food ingredient by the analysis of

cytotoxicity and genotoxicity. Food Res. Int. 100, 791–797. https://doi.org/10.1016/J.FOODRES.2017.08.012.
Janissen, B., Huynh, T., 2018. Chemical composition and value-adding applications of coffee industry by-products: a review. Resour. Conserv. Recycl. 128, 110–117.
Jastroch, M., Divakaruni, A.S., Mookerjee, S., Treberg, J.R., Brand, M.D., 2010. Mitochondrial proton and electron leaks. Essays Biochem. 47, 53–67. https://doi.org/10.1042/bse0470053.
Jung, U.J., Choi, M.-S., 2014. Obesity and its metabolic complications: the role of adipokines and the relationship between obesity, inflammation, insulin resistance, dyslipidemia and nonalcoholic fatty liver disease. Int. J. Mol. Sci. 15, 6184–6223. https://doi.org/10.3390/ijms15046184.
Kang, Y.E., Kim, J.M., Joung, K.H., Lee, J.H., You, B.R., Choi, M.J., Ryu, M.J., Ko, Y.B., Lee, M.A., Lee, J.H., Ku, B.J., Shong, M., Lee, K.H., Kim, H.J., 2016. The roles of adipokines, proinflammatory cytokines, and adipose tissue macrophages in obesity-associated insulin resistance in modest obesity and early metabolic dysfunction. PLoS One 11, e0154003. https://doi.org/10.1371/journal.pone.0154003.
Kim, A.-R., Yoon, B.K., Park, H., Seok, J.W., Choi, H., Yu, J.H., Choi, Y., Song, S.J., Kim, J.-W., 2016. Caffeine inhibits adipogenesis through modulation of mitotic clonal expansion and the AKT/GSK3 pathway in 3T3-L1 adipocytes. BMB Reports 49 (2), 111–115. https://doi.org/10.5483/bmbrep.2016.49.2.128.
Kobori, M., Takahashi, Y., Sakurai, M., Akimoto, Y., Tsushida, T., Oike, H., Ippoushi, K., 2016. Quercetin suppresses immune cell accumulation and improves mitochondrial gene expression in adipose tissue of diet-induced obese mice. Mol. Nutr. Food Res. 60, 300–312. https://doi.org/10.1002/mnfr.201500595.
Lagoa, R., Graziani, I., Lopez-Sanchez, C., Garcia-Martinez, V., Gutierrez-Merino, C., 2011. Complex I and cytochrome c are molecular targets of flavonoids that inhibit hydrogen peroxide production by mitochondria. Biochim. Biophys. Acta Bioenerg. 1807, 1562–1572. https://doi.org/10.1016/J.BBABIO.2011.09.022.
Lang, R., Dieminger, N., Beusch, A., Lee, Y.-M., Dunkel, A., Suess, B., Skurk, T., Wahl, A., Hauner, H., Hofmann, T., 2013. Bioappearance and pharmacokinetics of bioactives upon coffee consumption. Anal. Bioanal. Chem. 405 (26), 8487–8503. https://doi.org/10.1007/s00216-013-7288-0.
Langin, D., 2006. Adipose tissue lipolysis as a metabolic pathway to define pharmacological strategies against obesity and the metabolic syndrome. Pharmacol. Res. 53, 482–491. https://doi.org/10.1016/j.phrs.2006.03.009.
Lorenzo, M., Fernández-Veledo, S., Vila-Bedmar, R., Garcia-Guerra, L., De Alvaro, C., Nieto-Vazquez, I., 2008. Insulin resistance induced by tumor necrosis factor-α in myocytes and brown adipocytes12. J. Anim. Sci. 86, E94–E104. https://doi.org/10.2527/jas.2007-0462.
Lumeng, C.N., Deyoung, S.M., Saltiel, A.R., 2007. Macrophages block insulin action in adipocytes by altering expression of signaling and glucose transport proteins. Am. J. Physiol. Endocrinol. Metab. 292, E166–E174. https://doi.org/10.1152/ajpendo.00284.2006.
Luna-Vital, D., Weiss, M., Gonzalez de Mejia, E., 2017. Anthocyanins from purple corn ameliorated tumor necrosis factor-α-induced inflammation and insulin resistance in 3T3-L1 adipocytes via activation of insulin signaling and enhanced GLUT4 translocation. Mol. Nutr. Food Res. 61, 1700362. https://doi.org/10.1002/mnfr.201700362.
Magoni, C., Bruni, I., Guzzetti, L., Dell'Agli, M., Sangiovanni, E., Piazza, S., Regonesi, M.E., Maldini, M., Spezzano, R., Caruso, D., Labra, M., 2018. Valorizing coffee pulp by-products as anti-inflammatory ingredient of food supplements acting on IL-8 release. Food Res. Int. 112, 129–135. https://doi.org/10.1016/J.FOODRES.2018.06.026.
McArdle, M.A., Finucane, O.M., Connaughton, R.M., McMorrow, A.M., Roche, H.M., 2013. Mechanisms of obesity-induced inflammation and insulin resistance: insights into the emerging role of nutritional strategies. Front. Endocrinol. 4, 52. https://doi.org/10.3389/fendo.2013.00052.
Monteiro, R., Azevedo, I., 2010. Chronic inflammation in obesity and the metabolic syndrome. Mediat. Inflamm. 2010. https://doi.org/10.1155/2010/289645.
Morris, G.M., Huey, R., Lindstrom, W., Sanner, M.F., Belew, R.K., Goodsell, D.S., Olson, A.J., 2009. AutoDock4 and AutoDockTools4: automated docking with selective receptor flexibility. J. Comput. Chem. 30, 2785–2791. https://doi.org/10.1002/jcc.21256.
Murphy, M.P., 2009. How mitochondria produce reactive oxygen species. Biochem. J. 417, 1–13. https://doi.org/10.1042/BJ20081386.
Nardini, M., Cirillo, E., Natella, F., Scaccini, C., 2002. Absorption of phenolic acids in humans after coffee consumption. J. Agric. Food Chem. 50 (20). https://doi.org/10.1021/jf0257547.
Olefsky, J.M., Glass, C.K., 2010. Macrophages, inflammation, and insulin resistance. Annu. Rev. Physiol. 72, 219–246. https://doi.org/10.1146/annurev-physiol-021909-135846.
Ong, K.W., Hsu, A., Tan, B.K.H., 2012. Chlorogenic acid stimulates glucose transport in skeletal muscle via AMPK activation: a contributor to the beneficial effects of coffee on diabetes. PLoS One 7, e32718. https://doi.org/10.1371/journal.pone.0032718.
Paniagua, J.A., 2016. Nutrition, insulin resistance and dysfunctional adipose tissue determine the different components of metabolic syndrome. World J. Diabetes 7, 483–514. https://doi.org/10.4239/wjd.v7.i19.483.
Patti, M.-E., Corvera, S., 2010. The role of mitochondria in the pathogenesis of type 2 diabetes. Endocr. Rev. 31, 364–395. https://doi.org/10.1210/er.2009-0027.
Rebollo-Hernanz, M., Zhang, Q., Aguilera, Y., Martín-Cabrejas, M.A., Gonzalez de Mejia, E., 2019. Cocoa shell aqueous phenolic extract preserves mitochondrial function and insulin sensitivity by attenuating inflammation between macrophages and adipocytes *in vitro*. Mol. Nutr. Food Res. 63 (10), 1801413. https://doi.org/10.1002/mnfr.201801413.
Rector, R.S., Thyfault, J.P., Uptergrove, G.M., Morris, E.M., Naples, S.P., Borengasser, S.J., Mikus, C.R., Laye, M.J., Laughlin, M.H., Booth, F.W., Ibdah, J.A., 2010. Mitochondrial dysfunction precedes insulin resistance and hepatic steatosis and contributes to the natural history of non-alcoholic fatty liver disease in an obese rodent model. J. Hepatol. 52, 727–736. https://doi.org/10.1016/J.JHEP.2009.11.030.
Reilly, S.M., Saltiel, A.R., 2017. Adapting to obesity with adipose tissue inflammation. Nat. Rev. Endocrinol. 13, 633–643. https://doi.org/10.1038/nrendo.2017.90.
Sakamoto, T., Takahashi, N., Sawaragi, Y., Naknukool, S., Yu, R., Goto, T., Kawada, T., 2013. Inflammation induced by RAW macrophages suppresses UCP1 mRNA induction via ERK activation in 10T1/2 adipocytes. Am. J. Physiol. Cell Physiol. 304, C729–C738. https://doi.org/10.1152/ajpcell.00312.2012.
Sánchez-Patán, F., Monagas, M., Moreno-Arribas, M.V., Bartolomé, B., 2011. Determination of microbial phenolic acids in human faeces by UPLC-ESI-TQ MS. J. Agric. Food Chem. 59, 2241–2247. https://doi.org/10.1021/jf104574z.
Scazzocchio, B., Varì, R., Filesi, C., Del Gaudio, I., D'Archivio, M., Santangelo, C., Iacovelli, A., Galvano, F., Pluchinotta, F.R., Giovannini, C., Masella, R., 2015. Protocatechuic acid activates key components of insulin signaling pathway mimicking insulin activity. Mol. Nutr. Food Res. 59, 1472–1481. https://doi.org/10.1002/mnfr.201400816.
Schäffler, A., Schölmerich, J., 2010. Innate immunity and adipose tissue biology. Trends Immunol. 31, 228–235. https://doi.org/10.1016/j.it.2010.03.001.
Schoiswohl, G., Stefanovic-Racic, M., Menke, M.N., Wills, R.C., Surlow, B.A., Basantani, M.K., Sitnick, M.T., Cai, L., Yazbeck, C.F., Stolz, D.B., Pulinilkunnil, T., O'Doherty, R.M., Kershaw, E.E., 2015. Impact of Reduced ATGL-Mediated Adipocyte Lipolysis on Obesity-Associated Insulin Resistance and Inflammation in Male Mice. Endocrinology 156 (10), 3610–3624. https://doi.org/10.1210/en.2015-1322.
Shan, J., Fu, J., Zhao, Z., Kong, X., Huang, H., Luo, L., Yin, Z., 2009. Chlorogenic acid inhibits lipopolysaccharide-induced cyclooxygenase-2 expression in RAW264.7 cells through suppressing NF-κB and JNK/AP-1 activation. Int. Immunopharmacol. 9, 1042–1048. https://doi.org/10.1016/J.INTIMP.2009.04.011.
Shin, H.S., Satsu, H., Bae, M.-J., Zhao, Z., Ogiwara, H., Totsuka, M., Shimizu, M., 2015. Anti-inflammatory effect of chlorogenic acid on the IL-8 production in Caco-2 cells and the dextran sulphate sodium-induced colitis symptoms in C57BL/6 mice. Food Chem. 168, 167–175. https://doi.org/10.1016/J.FOODCHEM.2014.06.100.
Suganami, T., Nishida, J., Ogawa, Y., 2005. A paracrine loop between adipocytes and macrophages aggravates inflammatory changes. Arterioscler. Thromb. Vasc. Biol. 25, 2062–2068. https://doi.org/10.1161/01.ATV.0000183883.72263.13.
Szklarczyk, D., Morris, J.H., Cook, H., Kuhn, M., Wyder, S., Simonovic, M., Santos, A., Doncheva, N.T., Roth, A., Bork, P., Jensen, L.J., von Mering, C., 2017. The STRING database in 2017: quality-controlled protein–protein association networks, made broadly accessible. Nucleic Acids Res. 45, D362–D368. https://doi.org/10.1093/nar/gkw937.
Trott, O., Olson, A.J., 2010. AutoDock Vina: improving the speed and accuracy of docking with a new scoring function, efficient optimization, and multithreading. J. Comput. Chem. 31, 455–461. https://doi.org/10.1002/jcc.21334.
Wang, C.-H., Wang, C.-C., Huang, H.-C., Wei, Y.-H., 2013. Mitochondrial dysfunction leads to impairment of insulin sensitivity and adiponectin secretion in adipocytes. FEBS J. 280, 1039–1050. https://doi.org/10.1111/febs.12096.
Wang, S., Wang, X., Ye, Z., Xu, C., Zhang, M., Ruan, B., Wei, M., Jiang, Y., Zhang, Y., Wang, L., Lei, X., Lu, Z., 2015. Curcumin promotes browning of white adipose tissue in a norepinephrine-dependent way. Biochem. Biophys. Res. Commun. 466, 247–253. https://doi.org/10.1016/j.bbrc.2015.09.018.
Xu, X., Grijalva, A., Skowronski, A., van Eijk, M., Serlie, M.J., Ferrante, A.W., 2013. Obesity activates a program of lysosomal-dependent lipid metabolism in adipose tissue macrophages independently of classic activation. Cell Metabol. 18, 816–830. https://doi.org/10.1016/j.cmet.2013.11.001.
Yang, X., Zhang, X., Heckmann, B.L., Lu, X., Liu, J., 2011. Relative contribution of adipose triglyceride lipase and hormone-sensitive lipase to tumor necrosis factor-α (TNF-α)-induced lipolysis in adipocytes. The Journal of Biological Chemistry 286 (47), 40477–40485. https://doi.org/10.1074/jbc.M111.257923.
Ye, J., 2013. Mechanisms of insulin resistance in obesity. Front. Med. 7, 14–24. https://doi.org/10.1007/s11684-013-0262-6.
Yoneshiro, T., Matsushita, M., Hibi, M., Tone, H., Takeshita, M., Yasunaga, K., Katsuragi, Y., Kameya, T., Sugie, H., Saito, M., 2017. Tea catechin and caffeine activate brown adipose tissue and increase cold-induced thermogenic capacity in humans. Am. J. Clin. Nutr. 105 (4), 873–881. https://doi.org/10.3945/ajcn.116.144972.
Yoon, H.-Y., Lee, E.-G., Lee, H., Cho, I.J., Choi, Y.J., Sung, M.-S., Yoo, H.-G., Yoo, W.-H., 2013. Kaempferol inhibits IL-1β-induced proliferation of rheumatoid arthritis synovial fibroblasts and the production of COX-2, PGE2 and MMPs. Int. J. Mol. Med. 32, 971–977. https://doi.org/10.3892/ijmm.2013.1468.
Zebisch, K., Voigt, V., Wabitsch, M., Brandsch, M., 2012. Protocol for effective differentiation of 3T3-L1 cells to adipocytes. Anal. Biochem. 425, 88–90. https://doi.org/10.1016/J.AB.2012.03.005.
Zhang, J., Wang, X., Vikash, V., Ye, Q., Wu, D., Liu, Y., Dong, W., 2016. ROS and ROS-mediated cellular signaling. Oxid. Med. Cell. Longev. 2016https://doi.org/10.1155/2016/4350965. 4350965.